REACTOR POWER CALIBRATION

BY NOISE ANALYSIS

by

JESUS LOPEZ-COTARELO VILLAAMIL

Perito Industrial, Escuela Tecnica de Madrid, 1961

A MASTER'S THESIS

submitted in partial fulfillment of the

requirements for the degree

MASTER OF SCIENCE

Department of Nuclear Engineering

KANSAS STATE UNIVERSITY

Manhattan, Kansas

1968

Approved by:

Major Professor

TABLE OF CONTENTS

LIST OF TABLES

LIST OF FIGURES

NOMENCLATURE

A	Macroscopic cross section for all non-productive neutron absorption including leakage
C_i	Delayed neutron precursor population corresponding to the i^{th} group
C_{io}	Steady state component of the delayed neutron precursor population corresponding to the i^{th} group
$C_i(f)$	Fluctuating component of the delayed neutron precursor population corresponding to the i^{th} group as a function of frequency
$C_i(t)$	Fluctuating component of the delayed neutron precursor population corresponding to the i^{th} group as a function of time
D	Dispersion of a statistical distribution
e	Charge carried by each electron in coulombs
f	Frequency
f_b	Prompt neutron break frequency
F	Macroscopic cross section for fission
$H(f)$	Instruments transfer function
$\bar{I}$	Average current passing through the detector
$I(f)$	Fluctuating current
$I_c(f)$	White noise component due to the statistic of the detection process
$I_p(f)$	Pile noise component due to reactor neutron population

$\langle \lvert I \rvert^2 \rangle$	Spectral density of the diode current noise per unit frequency
$\langle \lvert I_c(f) \rvert^2 \rangle$	Spectral density of $I_c(f)$
$\langle \lvert I_p(f) \rvert^2 \rangle$	Spectral density of $I_p(f)$
$\langle \lvert I_p(1) \rvert^2 \rangle$	Spectral density of $I_p(f)$ at a frequency low enough to make $\lvert T(f) \rvert^2$ equal to unity
$\langle \lvert I_p(\infty) \rvert^2 \rangle$	Spectral density of $I_p(f)$ at a frequency high enough to make $\lvert T(f) \rvert^2$ negligible
ℓ^*	Prompt neutron lifetime
$\bar{m}$	Average number of electrons flowing per second
$\bar{m}_i$	Average number of reactions of type i occurring per second in the reactor
n	Total number of neutrons in the reactor before fission
n'	Total number of neutrons in the reactor after fission
n	Sample size (number of cycles)
n_i	Normalized mean amplitude observed at the frequency ω_i
$n(f)$	Fluctuating component of the neutron population as a function of frequency
$n(t)$	Fluctuating component of the neutron population as a function of time
n_o	Steady state component of the neutron population
$\langle \lvert n(f) \rvert^2 \rangle$	Spectral density of n(f)
N	Number of data points
P	Number of adjustable parameters
P_N	Probability that N prompt neutrons will be produced in any one fission

q_i	Net number of neutrons produced in the occurrence of one nuclear reaction of type i
Q	Charge transferred per neutron absorbed
R	Rission rate
S	Source of neutrons
S(f)	Fluctuating component of the source of neutrons as a function of frequency
S(t)	Fluctuating component of the source of neutrons as a function of time
$<\|S_o(f)\|^2>$	Spectral density of the noise equivalent source in neutron^2 per second
t	Time, integration time
T(f)	Reactor zero power transfer function
$\|T(f)\|$	Modulus of the reactor zero power transfer function
W	Reactor power in watts
V	Voltage
α	Ratio of the delayed neutron fraction to the neutron lifetime
β	Total fraction of delayed neutrons
β_i	Delayed neutrons fraction corresponding to the i^{th} group
$\delta\rho$	Increment in reactivity
Δf	Frequency band
Γ	Width of a statistical distribution
ε	Detector efficiency
λ	Delayed neutrons decay constant
λ_i	Delayed neutrons decay constant of the i^{th} group
$\bar{\nu}$	Average number of neutrons, both prompt and delayed, produced per fission

Φ_i	Input power spectrum
Φ_0	Output power spectrum
ρ	Reactivity
σ	Standard deviation
σ^2	Variance
ω	Angular frequency

1.0 INTRODUCTION

The term noise has a rather misleading meaning, due partially to the fact that it is commonly used in many areas of science, engineering and medicine. In each of these fields, it has a somewhat different meaning, but all have the common origin in acoustics, where it is used to describe a sound lacking in musical quality. Noise has thus come to mean randomness as distinguished from regularity. It was in Communication Engineering where noise analysis theory found its first application and the required mathematical treatment was developed (5, 23, 30, 34, 42).

Applications of noise theory to reactors were not immediate, although it was obvious that statistical processes were in operation. The first published works were those of Hoffman (12) in 1946 and Courant and Wallace (10) in 1947, which treated the theory of fluctuations of the neutron density at low reactor powers. The application of noise analysis to reactors received a great impulse with the publication of the works of Moore in 1957 (24, 25, 26). In his works, Moore pointed out the considerable saving of work that can be obtained by using noise analysis techniques, instead of rod-oscillator experiments, in the determination of reactor transfer function.

Since then a considerable amount of work has been done in the application of noise analysis to reactors (1, 4, 8, 9, 29, 37, 38, 39, 40). This interest in reactor noise has not been limited to this country. Several works have been published overseas (11, 21, 32, 44).

Recently, noise analysis has become a favorite field for investigators and the number of publications has increased. Noise analysis has been applied to the determination of neutron lifetime, delayed neutrons parameters,

effects of a rolling sea on reactor dynamics, amount of Pu-239 present in a reactor, etc.

One of the most important applications of noise analysis is the determination of the reactor transfer function, and from this determination to calculate the reactor power level. The standard method to calculate the reactor power is by determining the neutron flux by irradiation of foils. In a power reactor another method is available, consisting of measuring the electrical power at the generator terminals and the reactor power is estimated by considering the efficiency of all the equipment. Noise analysis provides another method of solving this problem for power levels of the order of watts.

The purpose of the work reported here is to calculate the power of the Kansas State University TRIGA Mark II by noise analysis techniques. The determination of the reactor power by noise analysis essentially implies the calculation of the reactor transfer function. From the knowledge of the transfer function it is possible to determine the reactor break frequency. The accurate knowledge of this parameter is of prime importance in reactor kinetics.

2.0 THEORETICAL DEVELOPMENT

2.1 The Fission Process

The production of neutrons from the fission process is an event that occurs according to the laws of probabilities. An integral number of neutrons is emitted in each fission, yet, measurements of $\bar{\nu}$, the average number of neutrons per fission, do not give an integer.

There is in fact a probability distribution. Diven (14) found that for U-235, $\bar{\nu}$ is 2.47 $\pm$ 0.03 and $\overline{\nu^2}$, 7.32 $\pm$ 0.15, at a neutron energy of 80 Kev. Diven also measured the relative width of the distribution, Γ, defined as $\Gamma = \frac{\overline{\nu^2} - \bar{\nu}}{\bar{\nu}^2}$. The result was 0.795 $\pm$ 0.007. For a Poisson distribution this width should be unity.

Feyman, et al. (15), have determined the second moment in the distribution of the number of neutrons in the thermal fission of U-235 as being 7.8 $\pm$ 0.6. Leachman (22) has determined for the second moment a value of 7.2. A Poisson distribution of $\bar{\nu}$ would lead to a value of 8.75 for this second moment.

Frisch and Littler (17) have experimentally measured the neutron distribution emitted from U-235 in the Graphite Low Energy Experimental Pile, (GLEEP), at Harwell. They found the relative width of the distribution to be 1.21 $\pm$ 0.15. The discrepancy with the currently accepted value of 0.795 $\pm$ 0.007 was due to inaccuracies in the chamber efficiency, measurement of the total number of fissions per second in the reactor and in the zero-power transfer function. Nevertheless, Frisch and Littler pointed out that the experimental results fit the assumption of a Poisson distribution.

Terrell (36) has compiled the dispersion defined as $D = \overline{\nu^2} - \bar{\nu}^2$ and the width, for several nuclides, including U-235 and compared the experimental data with the theoretical values. He found that the experimental data

indicates that the distributions are narrower than the Poisson distribution, for which $D = \bar{\nu}$ and $\Gamma = 1$. Nevertheless, Terrell pointed out that a Poisson distribution is a reasonably good representation of the data.

From the foregoing discussion the assumption that the fission process in U-235 is random and that it follows a Poisson distribution seems fair.

Consistent with other similar works (24, 32, 44), it is assumed that Diven's values for $\bar{\nu}$ and Γ are reasonably representatives for the neutron energy spectrum in the core of the KSUTMII reactor.

2.2 Noise Equivalent Source

In most reactor physics works, neutrons are treated as a continuous fluid instead of discrete particles. Neutrons are discrete particles and the chain reaction is a statistical event. These two facts give rise to random fluctuations in reactor power levels, which are characterized by the term "pile noise". These fluctuations have been studied by several researchers (4, 10, 17, 21).

Cohn (9) has presented a simplified theory of "pile noise". The "pile noise" may be considered as arising from a random "noise equivalent" neutron source driving the reactor, which represents the fluctuations in the number of neutrons available to the reactor, caused by the natural statistical fluctuations in the rates of neutron absorption and fission. The characteristics of this source may be readily calculated using conventional random probability noise theory. The only processes contributing to the neutron balance in a reactor are fission, absorption and leakage. All of these processes are governed by the laws of statistics and are assumed to follow a Poisson distribution. The phenomenon of thermionic emission takes place in terms of

electrons which are discrete particles and are emitted at random times, and their distribution also follows the Poisson Law (18). Therefore, the noise in the reactor source is analogous to the noise in a thermionic device that is used to detect fluctuations in the neutron population of the pile.

The magnitude of the noise equivalent source may be obtained from the Schottky formula (8)(18), which is usually written

$$\langle |I|^2 \rangle = 2e^2\bar{m} \tag{1}$$

where $\langle |I|^2 \rangle$ is the spectral density of the diode current noise in amps^2-sec, e, the charge carried by each electron in coulombs, and $\bar{m}$ is the average number of electrons flowing per second.

In the case of neutrons producing different types of reactions and generating different numbers of neutrons, Eq. (1) becomes

$$\langle |S_o(f)|^2 \rangle = 2 \sum_{i=1}^{n} q_i^2 \bar{m}_i \tag{2}$$

where $\langle |S_o(f)|^2 \rangle$ is the spectral density of the noise equivalent source in neutrons^2 sec^{-1}, n is the number of types of reactions that may occur in a reactor, q_i is the net number of neutrons produced in the occurrence of reactions of type i, and $\bar{m}_i$ is the average number of reactions of type i occurring per second.

In the treatment that follows, one-group, space independent theory is used, and the fluctuations in neutron population are assumed to be small in comparison to the average. Further the assumption is made that the delayed neutron fraction, β, is small in comparison to unity.

All types of reactions which occur in a reactor and contribute to the noise equivalent source may be classified in two groups:

a) Non-productive absorption, including leakage

b) Fission giving rise to N prompt neutrons.

With the above assumption it is readily derived (Appendix A) that Eq. (2) can be written as:

$$\langle |S_o(f)|^2 \rangle = \frac{2n}{\ell^*} \left(\frac{\overline{\nu^2} - \bar{\nu}}{\bar{\nu}^2} \right) \tag{3}$$

where n is the number of neutrons in the reactor, ℓ^* is the prompt neutron lifetime, and $\bar{\nu}$ is the average number of neutrons produced in one fission.

2.3 Observation of Pile Noise

The pile noise must be observed in order to be meaningful. The observation is done by means of a neutron detector.

Let ε be the efficiency of the detector, defined as the fraction of all neutrons absorbed in the reactor, and Q, the charge transferred per neutron absorbed; thus, $\bar{I}$, the average current passing through the detector, will be given by:

$$\bar{I} = \varepsilon Q \frac{n}{\ell^*}. \tag{4}$$

Superimposed on this steady current there will be fluctuation currents which arise in two ways:

a) Fluctuation currents will be produced by the pile noise fluctuations in the reactor neutron population to which the detector is exposed

b) The steady current $\bar{I}$, is made up of many pulses of current produced by randomly arriving neutrons; thus there will be a white noise component due to the statistics of this detection process.

The pile noise fluctuations of part a) is obtained by calculating the spectral density of the average current $\bar{I}$ and is given by

$$\langle |I_p(f)|^2 \rangle = \left(\frac{\varepsilon Q}{\ell^*}\right)^2 \langle |n(f)|^2 \rangle . \tag{5}$$

By substitution of Eq. (B-18), (Appendix B), the following is obtained:

$$\langle |I_p(f)|^2 \rangle = \frac{2n\varepsilon^2 Q^2}{\ell^*[(2\pi fL)^2 + B^2]} \left(\frac{\overline{\nu^2} - \bar{\nu}}{\bar{\nu}^2}\right). \tag{6}$$

Considering Eq. (B-16), Eq. (6) can be written as

$$\langle |I_p(f)|^2 \rangle = \frac{2n\varepsilon^2 Q^2}{\ell^{*3}} |T(f)|^2 \frac{\overline{\nu^2} - \bar{\nu}}{\bar{\nu}^2} . \tag{7}$$

The spectral density of the white noise component of part b) is obtained by the use of Eq. (1) with $e = Q$ and $\bar{m} = \frac{n\varepsilon}{\ell^*}$.

Thus:

$$\langle |I_c(f)|^2 \rangle = 2Q^2 \left(\frac{\varepsilon n}{\ell^*}\right) = 2Q\bar{I}. \tag{8}$$

If $\varepsilon << 1$, the two noise components of the spectral density are first order and are uncorrelated. The total current noise in the detector output is then the sum of the aforementioned noise components, i.e.,

$$\langle |I(f)|^2 \rangle = \langle |I_p(f)|^2 \rangle + \langle |I_c(f)|^2 \rangle . \tag{9}$$

By substitution of Eqs. (7) and (8)

$$\langle |I(f)|^2 \rangle = 2Q^2 \frac{\varepsilon n}{\ell^*} \left[1 + \frac{\varepsilon}{(2\pi fL)^2 + B^2} \left(\frac{\overline{\nu^2} - \bar{\nu}}{\bar{\nu}^2}\right)\right] \tag{10}$$

that alternatively can be written as

$$\langle |I(f)|^2 \rangle = 2Q^2 \frac{\varepsilon n}{\ell^*} \left[1 + \frac{\varepsilon}{\ell^{*2}} |T(f)|^2 \left(\frac{\overline{\nu^2} - \bar{\nu}}{\bar{\nu}^2}\right)\right]. \tag{11}$$

Thus, the relative proportion of pile noise to white noise in the detector output depends on the detector efficiency.

The type of noise spectrum described by Eq. (11) has been experimentally observed in a number of reactors (8). It is identical to expressions derived by other investigators (10, 17) who have used different methods of analysis to explain the results of noise or statistical experiments in reactors (15).

2.4 Derivation of Expressions for ε and Q

Two important parameters required for the calculation of the reactor power are the detector efficiency and the charge transferred per neutron absorbed.

Schröder (32) has derived a method to determine ε and Q by noise analysis techniques.

In the graphical representation of the modulus of the zero-power transfer function, $|T(f)|^2$ versus frequency there is an extended range of frequencies for which $|T(f)|^2$ is reasonably constant. In the case of U-235 fueled

reactors this range is around frequencies of 1 cps. For U-235 reactors, the delayed neutron fraction is of the order of 8.2×10^{-3} and ℓ^* is of the order of 7.5×10^{-5} secs. Consequently, β/ℓ^* is of the order of 100 secs^{-1}.

For frequencies much less than 100 cps, i.e., around 1 cps, Eqs. (B-13) and (B-14) become respectively:

$$L = \ell^* \tag{12}$$

$$B = \beta. \tag{13}$$

By substitution into (B-15), the modulus of the transfer function becomes, for low frequencies,

$$|T(f)|^2 \sim \frac{\ell^{*2}}{\beta^2} \tag{14}$$

as $(2\pi f)^2$ can be neglected in comparison with (β/ℓ^*).

Therefore Eq. (10) becomes, for low frequencies,

$$\langle |I(1)|^2 \rangle = \frac{2Q^2\varepsilon n}{\ell^*} \left[1 + \frac{\varepsilon}{\beta^2} \frac{\overline{\nu^2} - \bar{\nu}}{\bar{\nu}^2}\right] \tag{15}$$

where $\langle |I(1)|^2 \rangle$ represents the spectral density of the current through the detector at frequencies around 1 cps.

For sufficiently high frequencies, i.e., above 100 cps., the second term of Eq. (10) becomes negligible, because it is proportional to ω^{-2}.

Thus for high frequencies

$$\langle |I(\infty)|^2 \rangle = 2Q^2\varepsilon \frac{n}{\ell^*} \tag{16}$$

where $\langle|I(\infty)|^2\rangle$ has the meaning of the spectral density of the current through the chamber at high frequencies.

Substitution of Eq. (16) into (15) and solving for ε gives

$$\varepsilon = \frac{\beta^2}{\frac{\overline{\nu^2} - \bar{\nu}}{\bar{\nu}^2}} \frac{\langle|I(1)|^2\rangle - \langle|I(\infty)|^2\rangle}{\langle|I(\infty)|^2\rangle} . \tag{17}$$

Combining Eqs. (4) and (16) an expression for Q is obtained, i.e.,

$$Q = \frac{1}{2\bar{I}} \langle|I(\infty)|^2\rangle. \tag{18}$$

Diven (12) gives for thermal fission in U-235 the following values:

$$\bar{\nu} = 2.47 \pm 0.03$$

$$\overline{\nu^2} = 7.32 \pm 0.15$$

$$\frac{\overline{\nu^2} - \bar{\nu}}{\bar{\nu}^2} = 0.795 \pm 0.007$$

Substitution of the above values into Eq. (17) gives

$$\varepsilon = 1.257\ \beta^2 \frac{\langle|I(1)|^2\rangle - \langle|I(\infty)|^2\rangle}{\langle|I(\infty)|^2\rangle} . \tag{19}$$

Q and ε can be calculated from Eqs. (18) and (19), respectively, by measurement of two spectral densities, at well determined and properly selected frequencies and by the determination of the delayed neutrons fraction. In a later section the determination of β, the delayed neutrons fraction, is discussed.

2.5 Determination of the Reactor Power Level

Using the theory developed in the previous sections it is possible to derive an expression for the power of the reactor as a function of the average current through the detector, $\bar{I}$, the detector efficiency, ε, and the charge produced per neutron absorbed in the detector, Q.

When the frequency is very high compared to the decay constants, λ_i, of the delayed neutrons precursors it is found from Eqs. (B-13) and (B-14) that

$$L = \ell^* \tag{20}$$

and

$$B = \beta. \tag{21}$$

Therefore Eq. (6) becomes

$$\langle |I_p(f)|^2 \rangle = \frac{2n\varepsilon^2 Q^2}{\ell^*[(2\pi f\ell^*)^2 + \beta^2]} \frac{\overline{\nu^2} - \bar{\nu}}{\bar{\nu}^2} . \tag{22}$$

Dividing Eq. (22) by the square of the average current through the detector given by (4), it is obtained that

$$\frac{\langle |I_p(f)|^2 \rangle}{\bar{I}^2} = \frac{2\ell^*}{n[(2\pi f\ell^*)^2 + \beta^2]} \frac{\overline{\nu^2} - \bar{\nu}}{\bar{\nu}^2} . \tag{23}$$

The prompt neutron break frequency is

$$f_b = \frac{\beta}{2\pi\ell^*} . \tag{24}$$

In the region where the frequency is low compared with β/ℓ^* Eq. (23) becomes

$$\frac{\langle |I_p(f)|^2 \rangle}{\bar{I}^2} = \frac{1}{n/\ell^*} \frac{2}{\beta^2} \frac{\overline{\nu^2} - \bar{\nu}}{\bar{\nu}^2} \tag{25}$$

The quantity n/ℓ^* indicates the number of neutrons that undergo productive or unproductive absorption per unit time (including leakage of neutrons) and for a critical reactor is equal to the number of neutrons arising from fission.

Defining R as the mean number of fissions in the reactor per unit time or reaction rate

$$R = \frac{n}{\ell^*} \tag{26}$$

and the reactor power in watts is

$$W = R \frac{1}{3.1} \times 10^{-10}. \tag{27}$$

It is assumed that the fission rate is 3.1×10^{10} fissions/sec-watt.

Combining Eqs. (26) and (27) and by substitution into (25) gives

$$\frac{\langle |I_p(f)|^2 \rangle}{\bar{I}^2} = \frac{2}{3.1 \times 10^{10}} \frac{1}{\beta^2 W} \frac{\overline{\nu^2} - \bar{\nu}}{\bar{\nu}^2}. \tag{28}$$

In the region where the frequency is low compared with β/ℓ^*, the spectral density of the average current through the detector $\langle |I_p(f)|^2 \rangle$, given by (6) becomes

$$\langle |I_p(f)|^2 \rangle = \frac{2n\varepsilon^2 Q^2}{\ell^* \beta^2} \frac{\overline{\nu^2} - \bar{\nu}}{\bar{\nu}^2}. \tag{29}$$

Combining Eqs. (4), (28) and (29) and solving for W gives

$$W = 3.23 \times 10^{-11} \frac{\bar{I}}{Q \cdot \varepsilon}, \tag{30}$$

where W is in watts, $\bar{I}$ is in amperes and Q is in coulombs.

Schröder (32) has derived another method to determine the reactor power level, using the spectral densities of the current through the detector at low and high frequencies, namely, $\langle|I(1)|^2\rangle$ and $\langle|I(\infty)|^2\rangle$.

Solving Eq. (4) for Q, and by substitution into Eq. (15) gives

$$\langle|I(1)|^2\rangle = 2\bar{I}^2 \frac{\ell^*}{n} \left[\frac{1}{\varepsilon} + \frac{1}{\beta^2} \frac{\overline{\nu^2} - \bar{\nu}}{\bar{\nu}^2}\right]. \tag{31}$$

From Eqs. (4) and (16) gives

$$\langle|I(\infty)|^2\rangle = 2 \frac{\bar{I}^2}{\varepsilon} \frac{\ell^*}{n} . \tag{32}$$

By proper operations with Eqs. (31) and (32) it is derived

$$\frac{n}{\ell^*} = \frac{2}{\beta^2} \frac{\overline{\nu^2} - \bar{\nu}}{\bar{\nu}^2} \frac{\bar{I}^2}{\langle|I(1)|^2\rangle - \langle|I(\infty)|^2\rangle} \tag{33}$$

which jointly with Eqs. (26) and (27) gives

$$W = 6.44 \times 10^{-11} \frac{1}{\beta^2} \frac{\overline{\nu^2} - \bar{\nu}}{\bar{\nu}^2} \frac{\bar{I}^2}{\langle|I(1)|^2\rangle - \langle|I(\infty)|^2\rangle} \tag{34}$$

and by substitution of the values given by Diven (14) finally it is obtained

$$W = 1.26 \times 10^{-10} \frac{\bar{I}^2}{\beta^2} \frac{1}{\langle|I(1)|^2\rangle - \langle|I(\infty)|^2\rangle}. \tag{35}$$

The above equation gives the power of the reactor in watts as a function of the average current through the detector, $\bar{I}$, the spectral densities of I at two well determined and properly selected frequencies and as a function of the delayed neutron fraction β.

2.6 Determination of the Break Frequency

One important parameter in reactor kinetics is the break frequency, α. Usually the break frequency is calculated by the Rossi-alpha experiment in which the ratio $\alpha = \beta/\ell^*$ is determined. Typical of the many Rossi-alpha experiments is that of Orndoff (28) on the Godiva-I reactor. In a similar manner Brunson (6) has determined β/ℓ^* for a number of ZPR-III cores. Cohn (8) has developed a method to measure the quotient β/ℓ^* by noise analysis principles. The high frequency rolloff portion of the reactor transfer function is strongly dependent on the quotient of the effective delayed neutron fraction over the prompt neutron lifetime.

The shape of the noise spectrum observed should be independent of the reactor power level. In practice, however, there are upper and lower limits to the power that may be used. It must be sufficiently high so that the pile noise is large compared with the background noise of the equipment but must not be so large that the chamber behaves improperly or the signal overrides the amplifier. Also the power level should be high enough so that the reactor is truly critical and not merely multiplying some extraneous or inherent source.

In the frequency range where the frequency is large compared to the delayed neutrons decay constants, the squared modulus of the zero-power transfer function is proportional to $\frac{1}{\alpha^2 + \omega^2}$, i.e.,

$$|T(f)|^2 \simeq \frac{1}{\alpha^2 + \omega^2} \tag{36}$$

where

$$\alpha = \beta/\ell^*. \tag{37}$$

The observed noise spectrum can be represented by the expression

$$A + \frac{B}{\alpha^2 + \omega^2} \tag{38}$$

where the first term is the white noise component and the second term is the pile noise component. Expression (38) is the function that is desired to be fit to the experimental data. The fitting is done by minimizing the least squares sum

$$S = \sum_{i=1}^{N} \left(n_i^2 - A - \frac{B}{\alpha^2 + \omega_i^2}\right)^2 \tag{39}$$

where n_i^2 is the normalized mean amplitude squared, observed at the angular frequency ω_i, and N is the number of data points.

The weight for each point is taken as unity, since the presence of other errors, such as reactor and instrument drifts tends to mask the statistical error of the fractional standard deviation of noise measurements and to make the standard error of all points about the same.

Differentiating Eq. (39) with respect to A, B, and α, and setting the derivatives equal to zero gives three equations in the three unknowns. Elimination of A and B gives an equation for α^2 of the form

$$F(\alpha^2, n_i^2, \omega_i^2) = 0 \tag{40}$$

that has to be solved for α^2 (Appendix C).

3.0 ANALYSIS OF DATA

3.1 General

There are two general methods to perform a noise analysis of a reactor. Noise recording and analysis falls in two categories:

1. Analog or continuous,
2. Digital or discrete.

The former involves the use of analog computers if done off-line, i.e., after reactor operation. If done on-line, i.e., during reactor operation, the term continuous is more appropriate because the electronic analyzers use the filters, amplifiers, and integrators that handle continuous functions of time. Digital data analysis is invariably done off-line because a digital computer is involved. It is quite possible that mixtures of analog and digital methods may be used in a single experiment. Which of these two approaches to data recording and analysis is used depends on many factors, the prime factor being the availability of equipment. It may be said that, in general, digital analysis requires an appreciable amount of digital computer time. For the above two reasons, continuous analysis of the reactor noise was chosen for the analysis of the data in this thesis. Details of the method are discussed below.

3.2 Transfer Function from Noise Measurements

If the reactor is assumed to be a linear system, then a simple relationship exists between the transfer function and the power spectrum (or power spectral density function) of the input, $\Phi_i(f)$, and output, $\Phi_o(f)$, i.e.:

$$\Phi_o(f) = |T(f)|^2 \cdot \Phi_i(f). \tag{41}$$

The power spectrum is defined as the limit of the total average power in a given band width of frequencies divided by the band width as the band width approaches zero. If the input power spectrum can be considered as a constant over the frequency range of interest (25) the output power spectrum is

$$\Phi_o(f) \approx (|T(f)|^2). \tag{42}$$

Thus the square of the amplitude of the reactor transfer function differs only by a constant from the power spectrum of the reactor noise.

Experimentally, the reactor fluctuations are converted into current fluctuations by means of a neutron detector and these fluctuations are passed through a band pass filter set about the frequency f_i. The a.c. component of the resulting signal is squared and integrated to obtain the average value. When the average value is divided by the band width, Φ_o at f_i is determined. Repeated at different frequencies this procedure generates the function $\Phi_o(f)$.

It is found, however, that when the noise spectrum of a reactor is measured, it consists of two portions, the first being the reactor noise, and the second being the white noise, resulting mainly from the statistics of the neutron collection in the detector. White noise is defined as a noise signal which contains equal contributions from all frequencies, at least over the frequency range of interest. The spectral density of white noise is a constant.

The instrumentation introduces noise which also has a characteristic spectral density. If the transfer function of the instrumentation system is H(f), then the measured output spectral density is given by

$$\Phi_o(f) = \{\Phi_n(f) + \Phi_i(f) \ |T(f)|^2\} \ |H(f)|^2 \tag{43}$$

where $\Phi_n(f)$ is the white noise spectral density.

For most cases, the instrumentation noise is assumed to be white and the instrumentation transfer function is assumed to be flat over the frequency range of interest. Since $\Phi_i(f)$ is also assumed to be constant then

$$\Phi_o(f) = A + B \left|T(f)\right|^2 \tag{44}$$

where A and B are constants.

3.3 Selection of the Effective Delayed Neutron Fraction and Prompt Neutron Lifetime

Schultz (33) has tabulated the delayed neutron fraction, β_i, and decay constants, λ_i, for U-235 (99.9%). The mean value for β for all the six groups is 0.0064 and the average decay constant $\bar{\lambda}$ is 1.79×10^{-2} $secs^{-1}$.

The sum $\sum_{i=1}^{6} \frac{\beta_i}{\lambda_i}$ varies somewhat from reactor to reactor because of the difference between the spectra of delayed neutrons and those of fission neutrons. The energy of delayed neutrons is 0.5 to 0.6 Mev, whereas that of fission neutrons is 2 Mev on the average. For TRIGA reactors that sum is taken as 0.110 sec (35).

Similarly it is necessary to make use of an effective delayed neutron fraction β_{eff}, that is, in general, higher than 0.0064, especially if the reactor is small and undermoderated. The reason is that in such a reactor the fast leakage is high, and the leakage of fission neutrons is therefore greater than that of the lower energy delayed neutrons. In TRIGA reactors it is found that $\beta_{eff} = 0.0079$ (35).

For low frequencies the equation

$$\frac{\beta_{eff}}{\lambda_{eff}} = \Sigma \frac{\beta_i}{\lambda_i} \tag{45}$$

is valid and with the above values $\bar{\lambda}_{eff} = 7.18 \times 10^{-3}$ sec^{-1}.

The prompt neutron lifetime, ℓ^*, is given by reference (35) as 6.5×10^{-5} sec.

3.4 Frequency Range To Be Analyzed

When a noise spectrum is being determined it is possible to define a range of frequencies of interest.

The characteristics of the squared modulus of the zero-power transfer function, $|T(f)|^2$, depend on the time constants. The transfer function has seven time constants: λ_i^{-1} for each of the six groups of delayed neutrons and ℓ^*/β. The smallest value of λ_i^{-1} is 0.332 secs (33), which gives a corresponding break frequency of $f_b = 0.48$ cps. Consequently, below 0.48 cps $|T(f)|^2$ depends strongly on the delayed neutron parameters. The seventh time constant, ℓ^*/β, gives a break frequency of $\alpha = 19.35$ cps with $\ell^* = 6.5 \times 10^{-5}$ secs (41) and $\beta_{eff} = 7.9 \times 10^{-3}$ (35). To determine ℓ^*/β in TRIGA reactors the optimum band of frequencies to investigate is the decade centered around 19.35 cps.

The length of the flat portion of the curve at mid frequencies depends on the distance between β/ℓ^* and the smallest λ_i^{-1} of the six groups of delayed neutrons. This flat portion is of interest in determining the detector efficiency, ε, (Eq. (20)). From the above calculations it is inferred that the flat portion lies in a frequency range from 0.48 to 19.35 cps.

At high frequencies, above 100 cps, the curve will level off to a constant value. This value is required for the calculation of both the detector efficiency, ε, and the charge transferred per neutron interaction, Q.

From the foregoing discussion the frequency range to investigate is limited from frequencies around 1 cps to 1000 cps.

3.5 Calculation of the Required Number of Cycles per Spectral Point

The major consideration in determining the length of recording time for obtaining a specific precision is that of taking a sample of sufficiently large size. An essential preliminary for determining the sample is to specify given boundaries of precision within which one desires to be confident that the sample must lie.

In the measurement of reactor noise the quantity which one is interested in measuring is the root mean square noise in a given band width about a certain spectral frequency. This root mean square value is the standard deviation of the sample.

The sample size, i.e., the number of cycles required at a given spectral frequency can be determined by relating the desired precision to a certain confidence level. Then, it follows, that if the required number of cycles of noise are obtained, one may neglect the probability of the error being greater than the specified amount.

It is shown (45) that the standard error of the standard deviation, (s.e.), is given by

$$(s.e.) = \frac{\sigma}{\sqrt{2n}} \tag{48}$$

where σ is the standard deviation of the sample and n is the sample size (number of cycles). Therefore it is possible to calculate n for a permitted error and a confidence level of 95%.

The analysis times with the required number of cycles for low and high frequencies are listed in Table I.

Table I. Required Analysis Time for a Predetermined Error.

Permitted Error %	Number of Cycles Required	Analysis Time (min) at 1 cps	Analysis Time (sec) at 100 cps
10	200.00	3.33	2.00
9	246.91	4.12	2.41
8	312.50	5.20	3.13
7	408.16	6.80	4.08
6	555.55	9.26	5.56
5	800.00	13.33	8.00
4	1250.00	20.83	12.50
3	2222.22	37.03	22.22
2	5000.00	83.33	50.00
1	20000.00	333.33	200.00

The data analysis at high frequencies does not present much inconvenience as regards to time. Such is not the case at low frequencies, where good precision represents a large amount of reactor operation time.

4.0 EXPERIMENTAL

4.1 Apparatus

The Kansas State University TRIGA Mark II reactor was used for power calibration. It was designed and engineered by General Atomic Company. The TRIGA Mark II reactor is a light-water moderated, graphite reflected reactor designed primarily for training and research. It has been designed for a continuous operation at a steady-state power level of 100 kw (thermal). For nuclear and engineering parameters of the KSUTMII reactor, the reader is referred to the currently available literature (35,41).

The TRIGA Mark II reactors have several experimental facilities, one of them being the central thimble. The central thimble, designed for experiments in the region of maximum flux and statistical weight, is a 1.33 inch inside diameter aluminum tube that extends from the top of the reactor pool to the bottom of the grid plate. A neutron ionization chamber, manufactured by Reuter-Stokes Electronic Components, Inc., Model RSN-229A, was used to detect the neutron population fluctuations. This ionization chamber uses boron enriched to 92% in B-10 as neutron sensitive material, and it is filled with a mixture of 95% Argon and 5% Nitrogen. The maximum chamber diameter is 1-1/32 inches and the maximum length 9-1/16 inches. The sensitive length is 7-1/2 inches and the sensitive area 192 cm^2. The reactivity worth of the chamber, when placed in the central thimble at approximately the core midplane, was 1 dollar.

The average current through the detector was measured by two different micro-micro-ammeters. One of them, a Keithley Model 410, manufactured by Keithley Instruments, Inc., was a line operated vacuum tube electrometer

designed especially for measuring small currents. It has a full scale range from 10^{-3} to 3×10^{-13} amperes. The accuracy of the ranges are: from 10^{-3} amperes through 3×10^{-7} amps within 2%, and from 10^{-8} through 3×10^{-13} within 4%. The KSU Nuclear Engineering inventory number is 818. The second used was a Model VTE-2 vacuum tube electrometer, manufactured by the Victoreen Instrument Company, with current ranges from 1×10^{-3} to 2×10^{-13} amperes, and it has an absolute accuracy of $\pm$ 3%. The Nuclear Engineering inventory number is 1316.

The frequency band was selected with a variable electronic band-pass filter, Model 330 R(R), manufactured by the Krohn-Hite Corporation. The frequency ranges covered by this instrument are from .02 cps to 2 kcps with upper and lower cut-off frequencies independently adjustable. The cut-off frequency calibration accuracy is within $\pm$ 5%. The minimum pass band width is obtained by setting the cut-off frequencies equal. In this case the lower 3 db point is at 0.77 times the cut-off frequency and the upper 3 db point is at 1.30 times the cut-off frequency. The spectral window width, Δf, is 0.53 f_o, where f_o is the cut-off frequency. The gain at the peak of the pass band filter is reduced by approximately 6 db. The Nuclear Engineering inventory number is 1269.

The electrical signal from the micro-micro ammeter was recorded in a magnetic tape recorder, Model 700/1400, manufactured by Technical Measurements Corporation. It is a multiple speed instrument, with speeds of 1-7/8, 3-3/4, 7-1/2 and 30 ips. The frequency response is from 0 to 2500 cps. The Nuclear Engineering inventory number is 1348.

A type RS dynograph recorder, manufactured by Beckman Instruments, Inc. was employed to record the output of the integrator. The KSU Nuclear Engineering inventory number is 733.

4.2 Experimental Procedure

4.2.1 Data Acquisition

In the acquisition of data the reactor power was raised to the power to be calibrated. The neutron detector was placed in the central thimble of the reactor at an elevation corresponding to the core midplane. The central thimble was chosen as the place to locate the neutron detector, as the reactor noise seen by the detector is greater in magnitude than the background of detector noise. In addition the reactor fluctuations were not damped out by the reflector and moderator, as would be the case if the detector were placed at some other reactor experimental facility. In the first attempt to obtain the reactor noise the detector was placed in the fast beam port, but the result was meaningless.

A second attempt was made with a neutron detector, encased in a polyethylene tube, placed in the central thimble. Water condensation and leakage made the detector current erratic. Finally a neutron ionization chamber designed to operate under water was used.

The electrical signal from the detector was fed into the micro-micro ammeter, where the total current was measured. The voltage signal from the micro-micro-ammeter was fed to the analog computer where the d.c. component was bucked out, the signal amplified within the 1 volt peak-to-peak tolerance of the tape recorder, and the signal recorded. Figure 1 shows the block diagram of this circuit. A detailed diagram of the analog computer circuitry is shown in Figure 2.

The reactor was operated at a certain power level for about 20 minutes while the reactor noise was recorded. The power levels attempted are listed

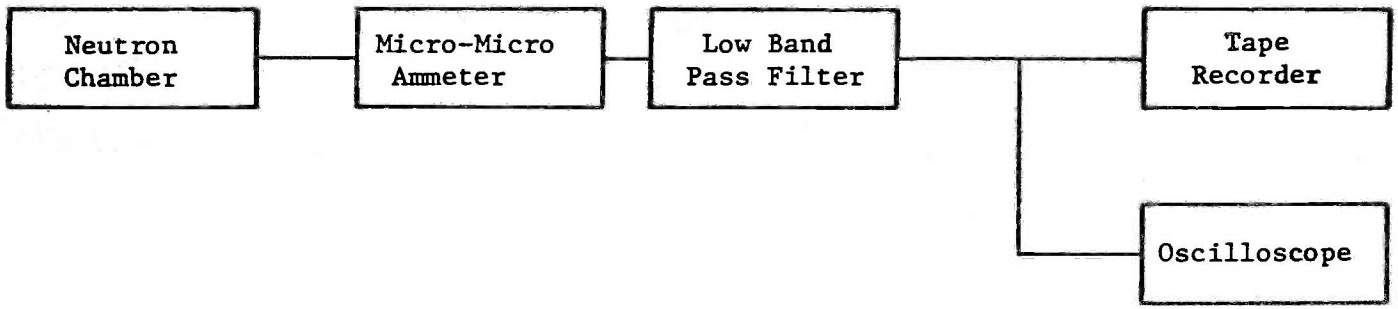

Figure 1. Instruments Block Diagram Used for Recording of Data.

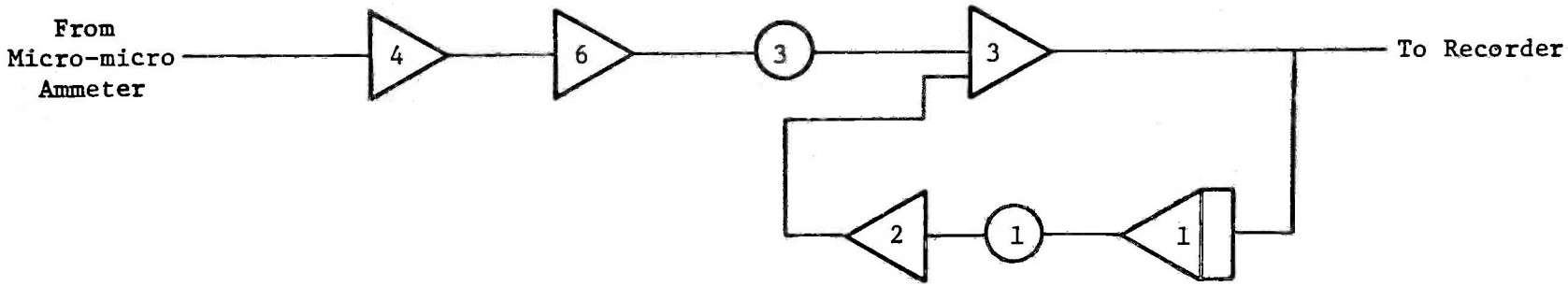

Figure 2. Schematic Diagram of Analog Computer Circuitry Used for Recording of Data.

in Table II. Of all the cases investigated a good recording of data was obtained only in cases 8, 10, 17, 18, 19 and 23. The reasons for this were multiple. Some of them are indicated above. Malfunction of the electronic equipment and experimenter's errors accounted for a few others.

Table II. Power Levels Investigated

Case No.	Console Indicated Power Level	Case No.	Console Indicated Power Level
1	1 w	13	100 w
2	1 w	14	200 w
3	1 w	15	500 w
4	1 w	16	1 kw
5	1 w	17	10 w
6	1 w	18	50 w
7	10 w	19	100 w
8	1 w	20	25 w
9	1 w	21	15 w
10	70 kw	22	20 w
11	20 w	23	15 w
12	50 w		

The main problem encountered in the acquisition of data was the difficulty of keeping the reactor at a steady power level for a minimum of twenty minutes. Movement of the control rod, required for keeping the reactor power at the proper level, introduced a noticeable perturbation in the recorded noise particularly in low frequencies, where good accuracy is of prime importance. This problem was attacked in several way such as changing the buck-out voltage, by-passing the portion of the tape which presented the

perturbation, etc. but without satisfactory results. Finally it was decided to allow the power to drift and not to move the control rods during recording of data. Nevertheless it was possible to obtain a reasonably steady power level at low power. The power drifts were monitored by observing the average current in the micro-micro-ammeter, at 1 minute intervals, and by post-recording analysis of the linear power log chart in the reactor console.

4.2.2 Data Analysis

Figure 3 shows the block diagram of the equipment employed for the analysis of data. The noise signal from the tape recorder was fed to the band pass filter to permit the analysis of only a narrow band of frequencies at a time. This was accomplished by setting the upper and lower cut-off frequencies equal to each other. The filtered signal was fed to the analog computer where it was squared and integrated. Figure 4 shows a detailed diagram of the analog computer circuitry. A part of this circuit was used as a high-pass filter to remove very low frequency components which pass through the filter and would appear as a d.c. drift. The integrated signal was fed to the strip chart recorder and the voltage read from the chart.

Figure 5 shows a specimen of the reactor noise at 15 watts. Figures 6, 7, and 8 are specimens of the reactor noise at three different frequencies, after it has been filtered through the frequency filter. Figures 9, 10 and 11 show the output of the integrator at 15 w and at 1.75, 5 and 10 cps.

The data were analyzed for a predetermined length of time to give a confidence level of 95% and a permitted error of 4%. This limit was chosen as a compromise between reactor operation time and a reasonable error. With the

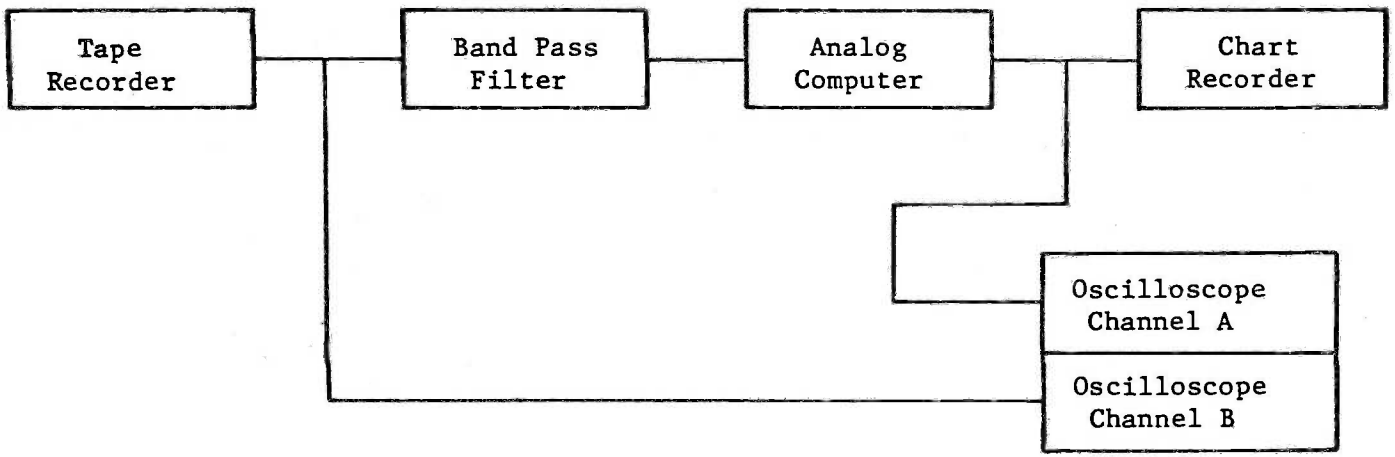

Figure 3. Instrument Block Diagram Used for Analysis of Data.

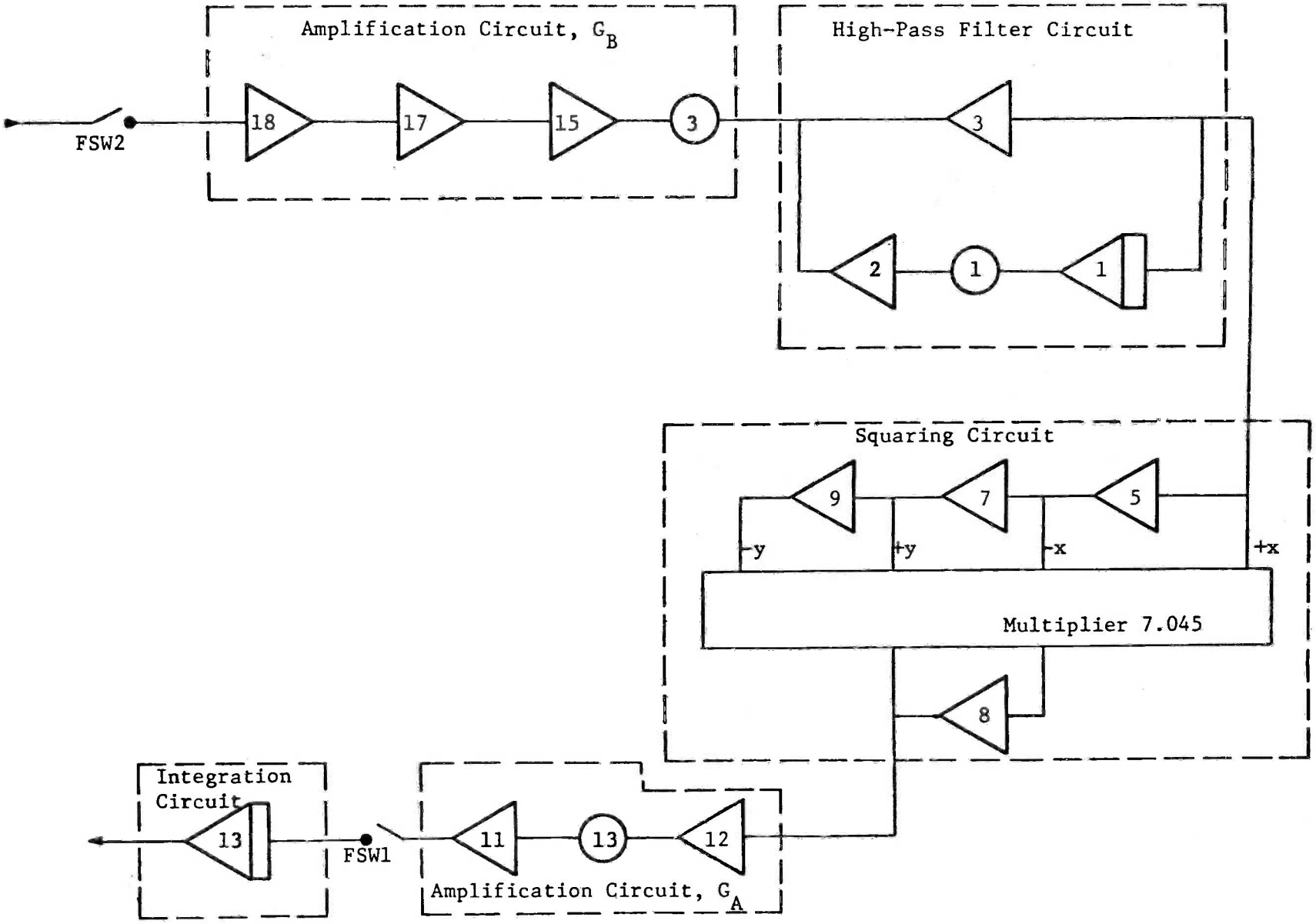

Figure 4. Schematic Diagram of Analog Computer Circuitry Used for Analysis of Data.

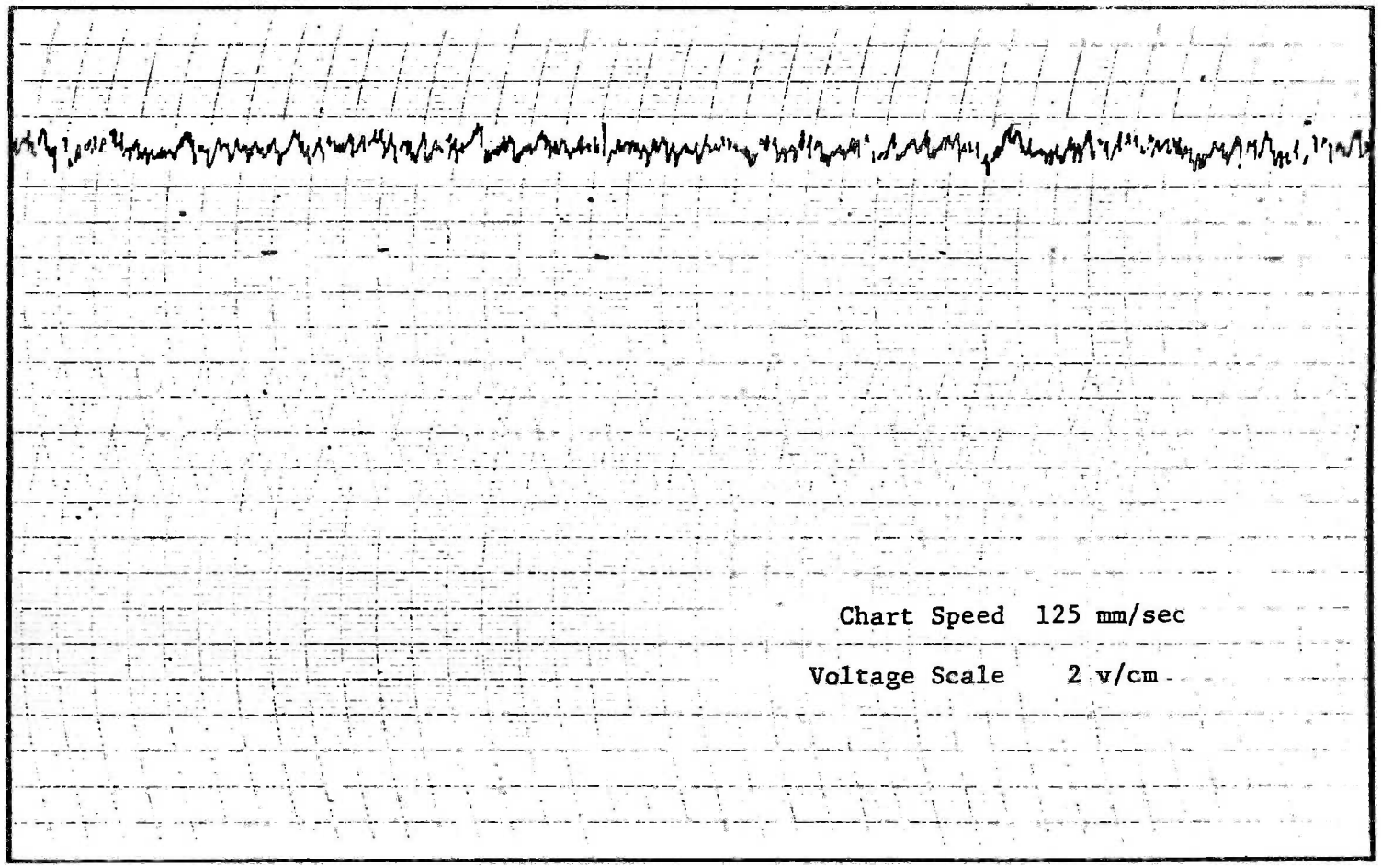

Figure 5. Specimen of Reactor Noise at 15 Watts. Full Spectrum.

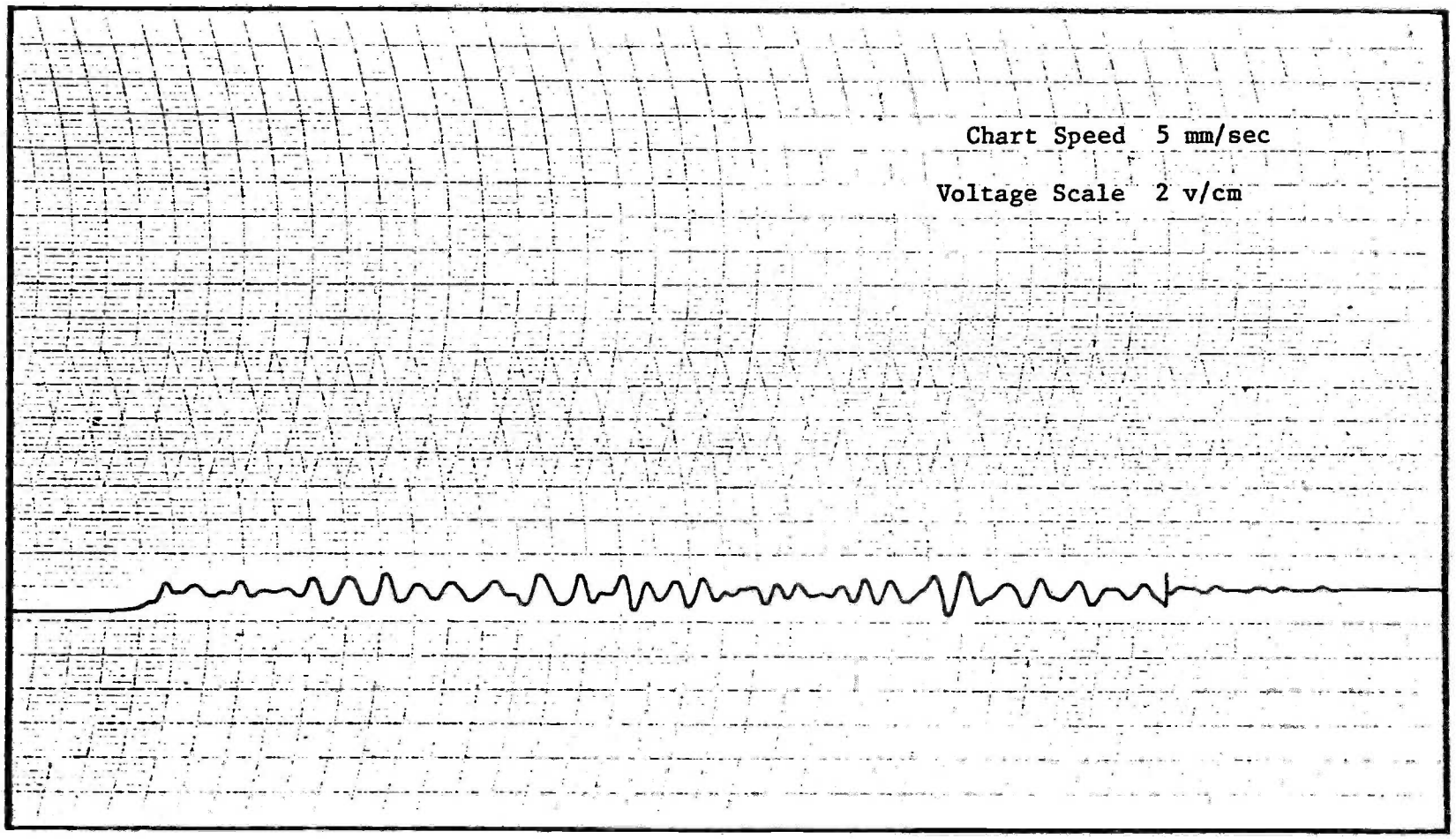

Figure 6. Specimen of Reactor Noise at 15 Watts. Frequency Filter at 1 cps.

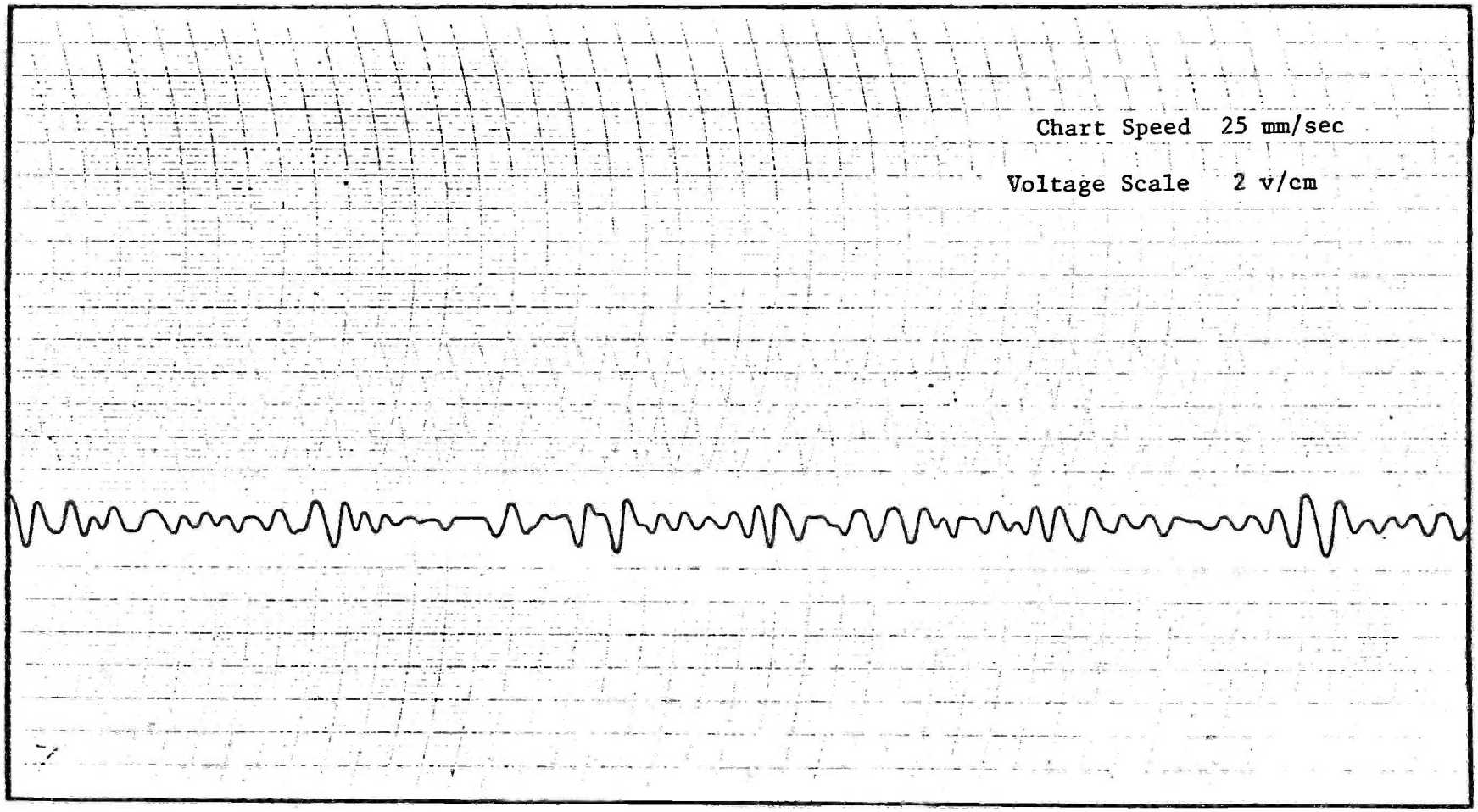

Figure 7. Specimen of Reactor Noise at 15 Watts. Frequency Filter at 5 cps.

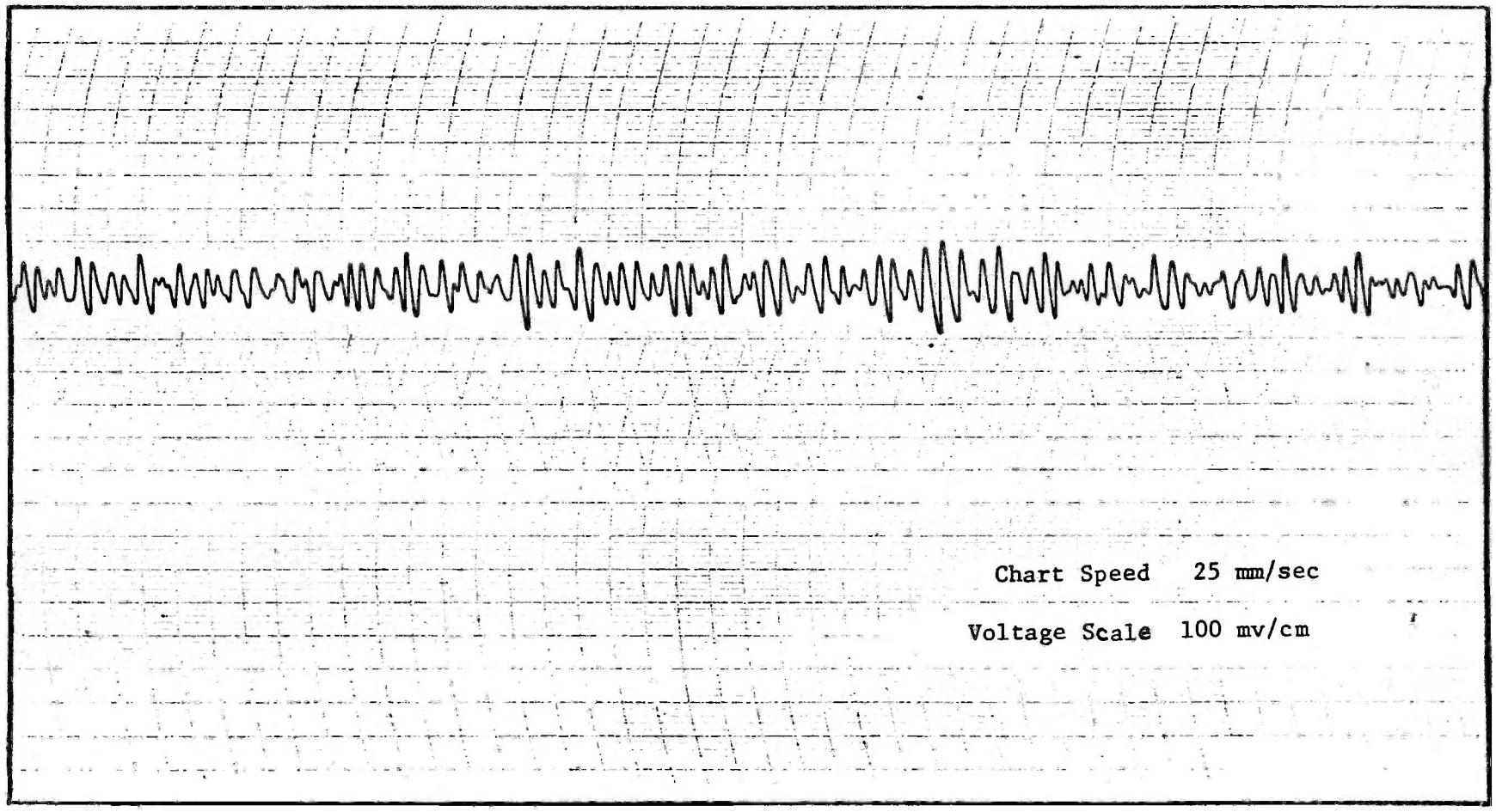

Figure 8. Specimen of Reactor Noise at 15 Watts. Frequency Filter at 10 cps.

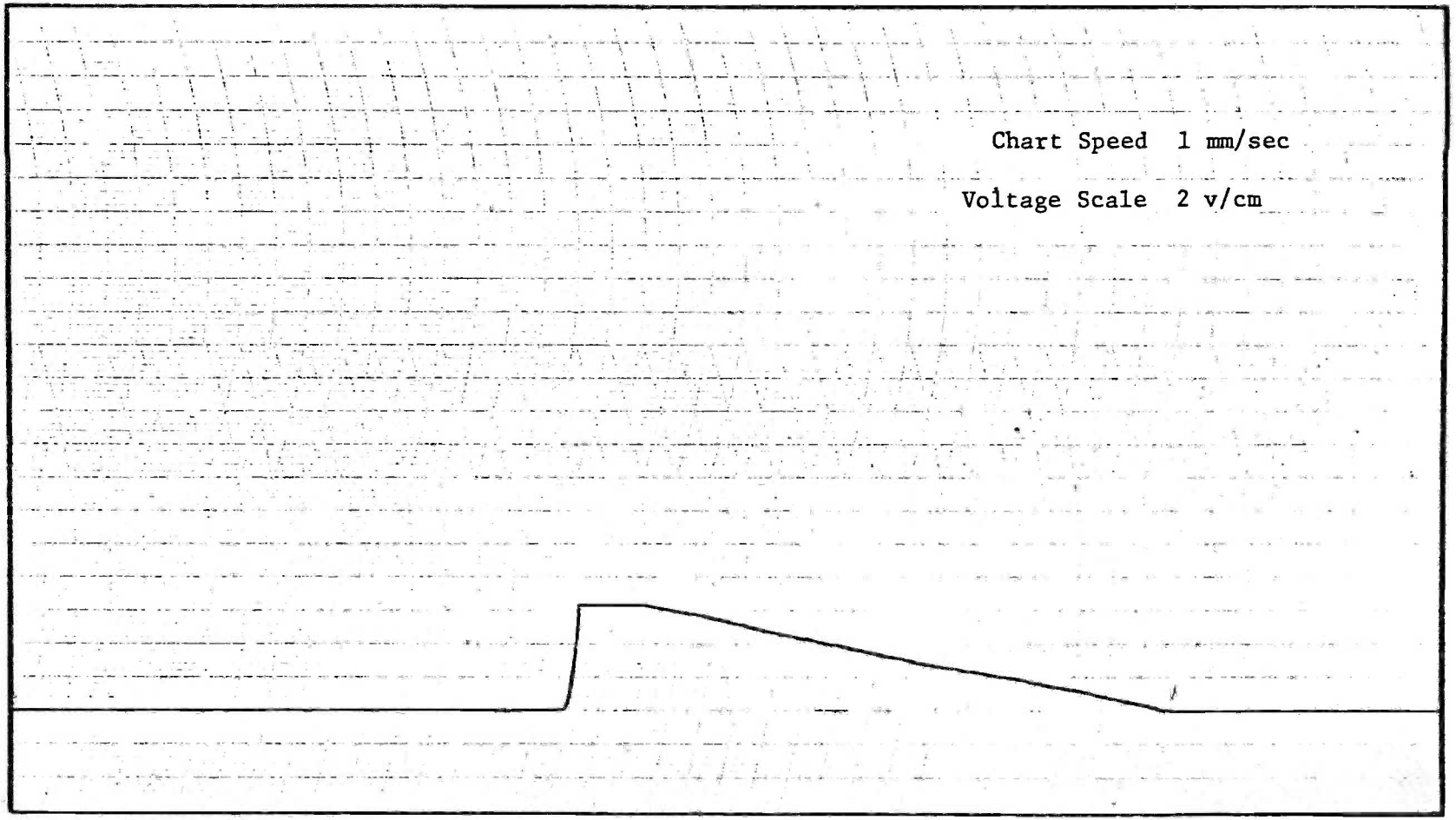

Figure 9. Specimen of Output of Integrator at 1.75 cps. Power Level 15 W.

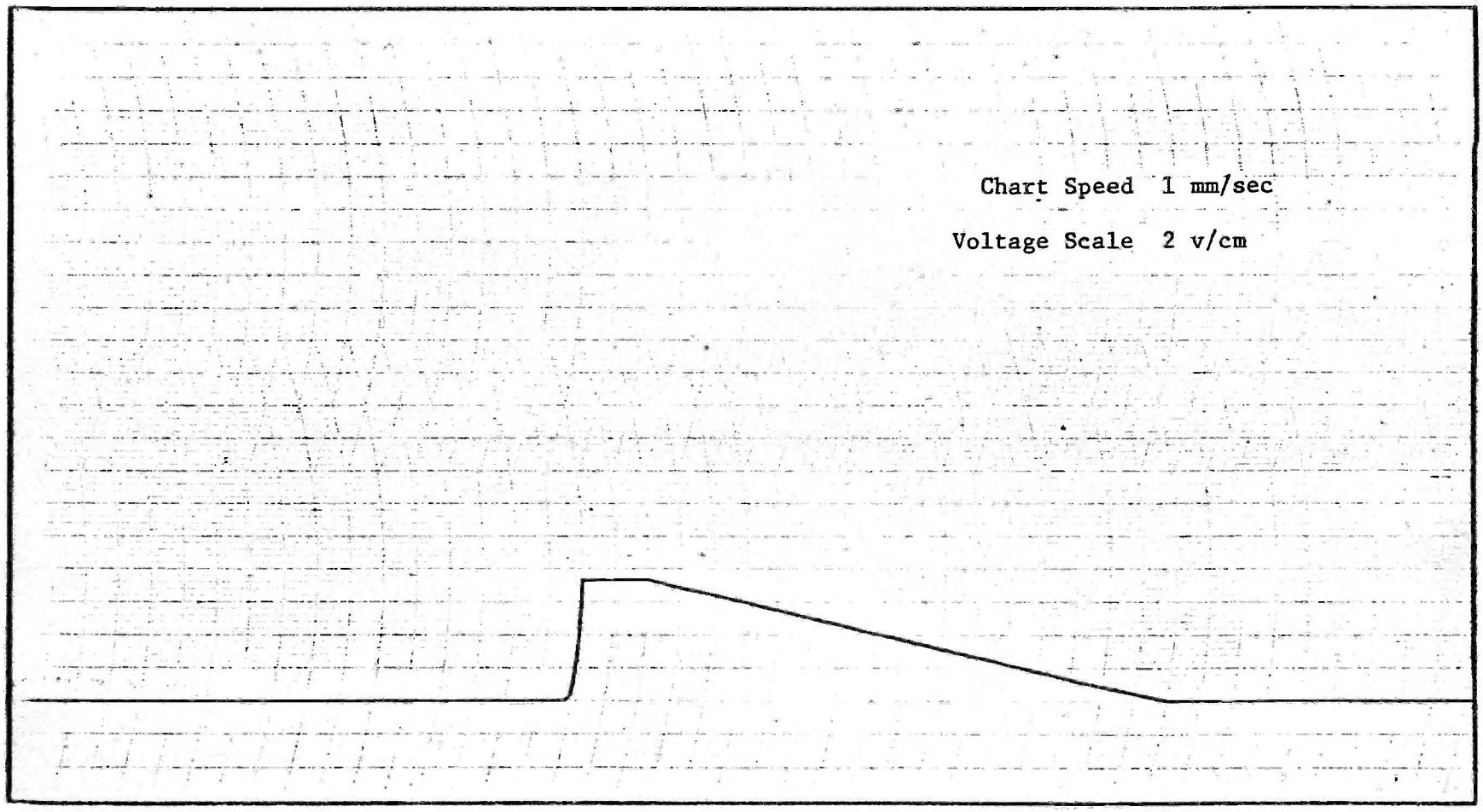

Figure 10. Specimen of Output of Integrator at 5 cps. Power Level 15 W.

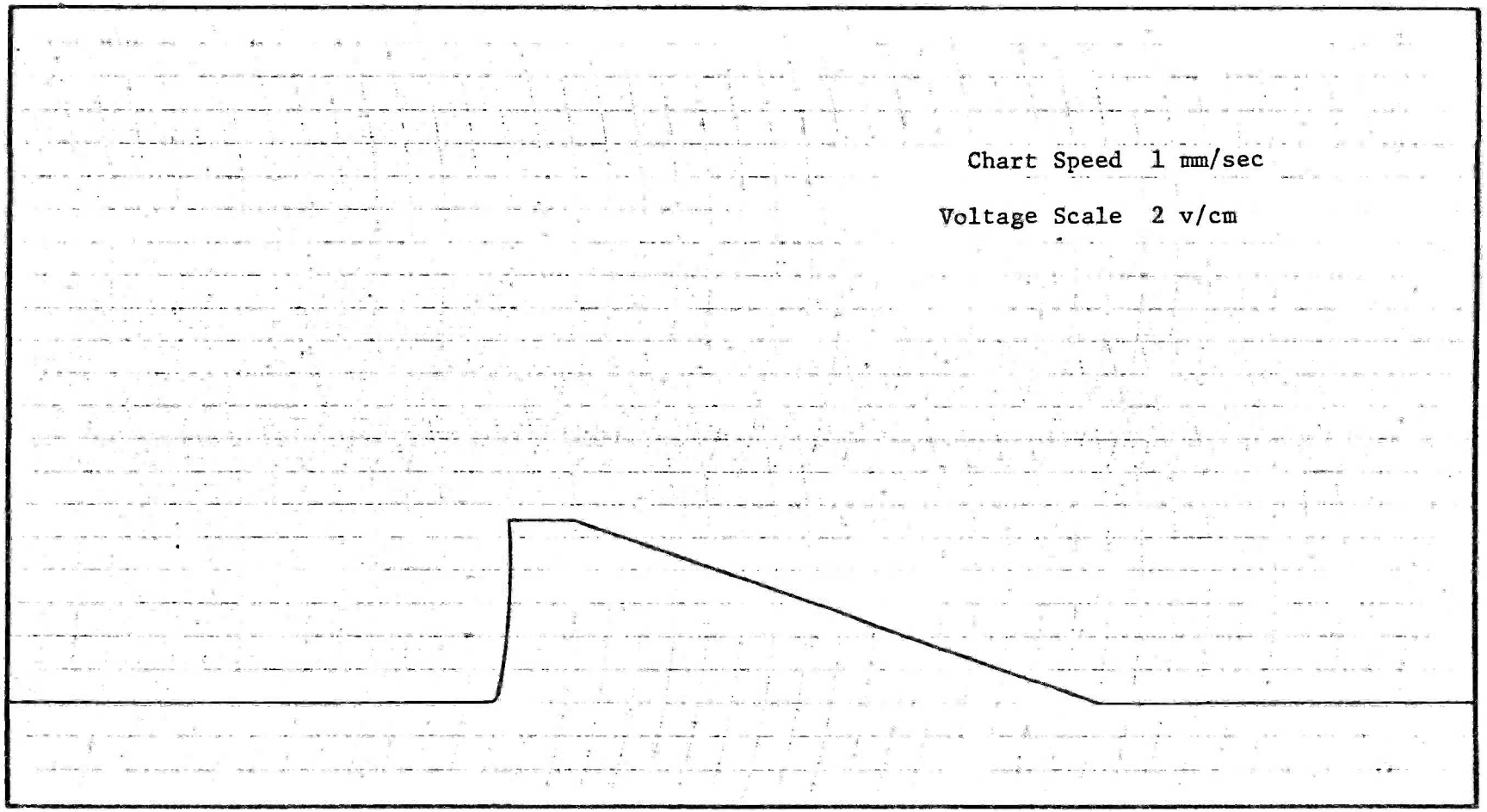

Figure 11. Specimen of Integrator Output at 10 cps. Power Level 15 W.

above limits the required number of cycles to be analyzed are obtained from (21)

$$\sigma + \frac{2\sigma}{\sqrt{2n}} = 1.04\ \sigma \tag{47}$$

where σ is the standard deviation of the sample and n the number of cycles. Solving the above equation, n = 1250. In Table III the analysis times in seconds at different frequencies are tabulated. As the required analysis time becomes very small at high frequencies, all frequencies above 60 cps were analyzed for 20 seconds.

Table III. Required Analysis Times at 4% Permitted Error

Frequency in cps	Time in seconds	Frequency in cps	Time in seconds
1	1250.0	30	41.7
1.1	1136.3	40	31.25
1.2	1041.6	50	25.0
1.4	892.9	60	20.8
1.6	781.3	70	17.9
1.8	694.4	80	15.6
2	625.0	100	12.5
3	416.7	120	10.4
4	312.5	140	8.9
6	208.3	160	7.8
8	150.3	180	6.9
10	125.0	200	6.3
12	104.2	250	5.0
14	89.3	300	4.2
16	78.1	400	3.1
18	69.4	600	2.1
20	62.5	800	1.6
		1000	1.3

The spectral power was obtained from the formula

$$\Phi_o(f) = \frac{V}{t \cdot f \cdot G_A \cdot G_B^2} \tag{48}$$

where V is the integrated voltage, t is the integration time in seconds, f is the frequency in cps, G_A is the analog computer amplification after squaring, and G_B the analog computer amplification before squaring.

The numerical calculations to obtain $\Phi_o(f)$ were performed on the IBM-1410 digital computer, with V, t, f, G_A and G_B as input data and $\Phi_o(f)$ obtained in arbitrary units and in decibels. A description and explanation of the computer code can be found in Appendix D.

The calibration of the system was accomplished by using a Krohn-Hite low frequency oscillator to feed a signal of known voltage and frequency into the analyzing circuit. The spectral power of this signal was calculated and the calibration based on the comparison of this number with that obtained from the reactor data.

5.0 DISCUSSION AND RESULTS

Figures 12 through 17 present the modulus of the transfer function, in decibels, versus frequency in cps for 1 w, 10 w, 15 w, 100 w and 70 kw respectively.

In these figures the presence of a large 60 cps component is noticeable due to instrumentation pick-up and grounding problems. The main contribution to this peak was caused by the micro-micro-ammeter, as can be seen by comparing Figures 13, 14, 16 and 17 with Figure 15. In the first case a Victoreen Model VT-2 electrometer was used and the 60 cps was quite large; in the second case, Figure 15, a Keithley micro-micro-ammeter was used and the peak was greatly reduced. This statement is supported by examination of the calibration curve, Figure 22, for the determination of which the micro-micro-ammeter was not used.

An analytical method was devised to remove this peak. It consisted in considering the spectral power $\Phi_o(f)$ to be made up of three components:

a) Reactor noise, which becomes negligible at high frequencies

b) White noise due to the statistics of neutron detection, which is constant through all the frequency range

c) A 60 cps noise due to instrumentation pick-up.

These three components are represented schematically in Figure 18.

The last component was due to a single frequency, 60 cps; therefore, the measured spectral power around this frequency would have the shape of the filter window as shown in Figure 19. This filter window was obtained by feeding a 60 cps wave of known amplitude through the analyzing circuit and calculating its spectral power. The 60 cps peak was removed by subtracting

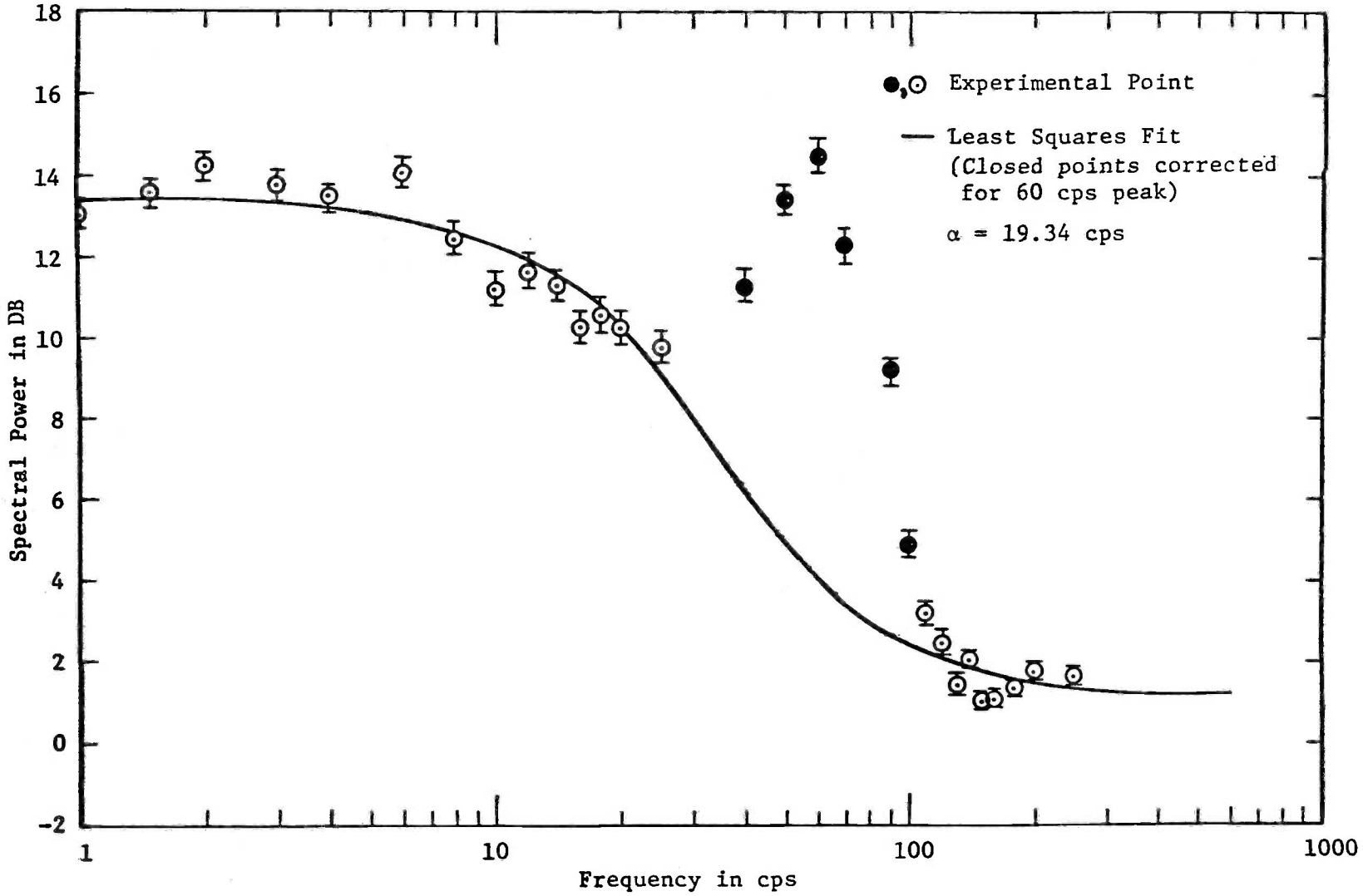

Figure 12. Spectral power at 1 watt.

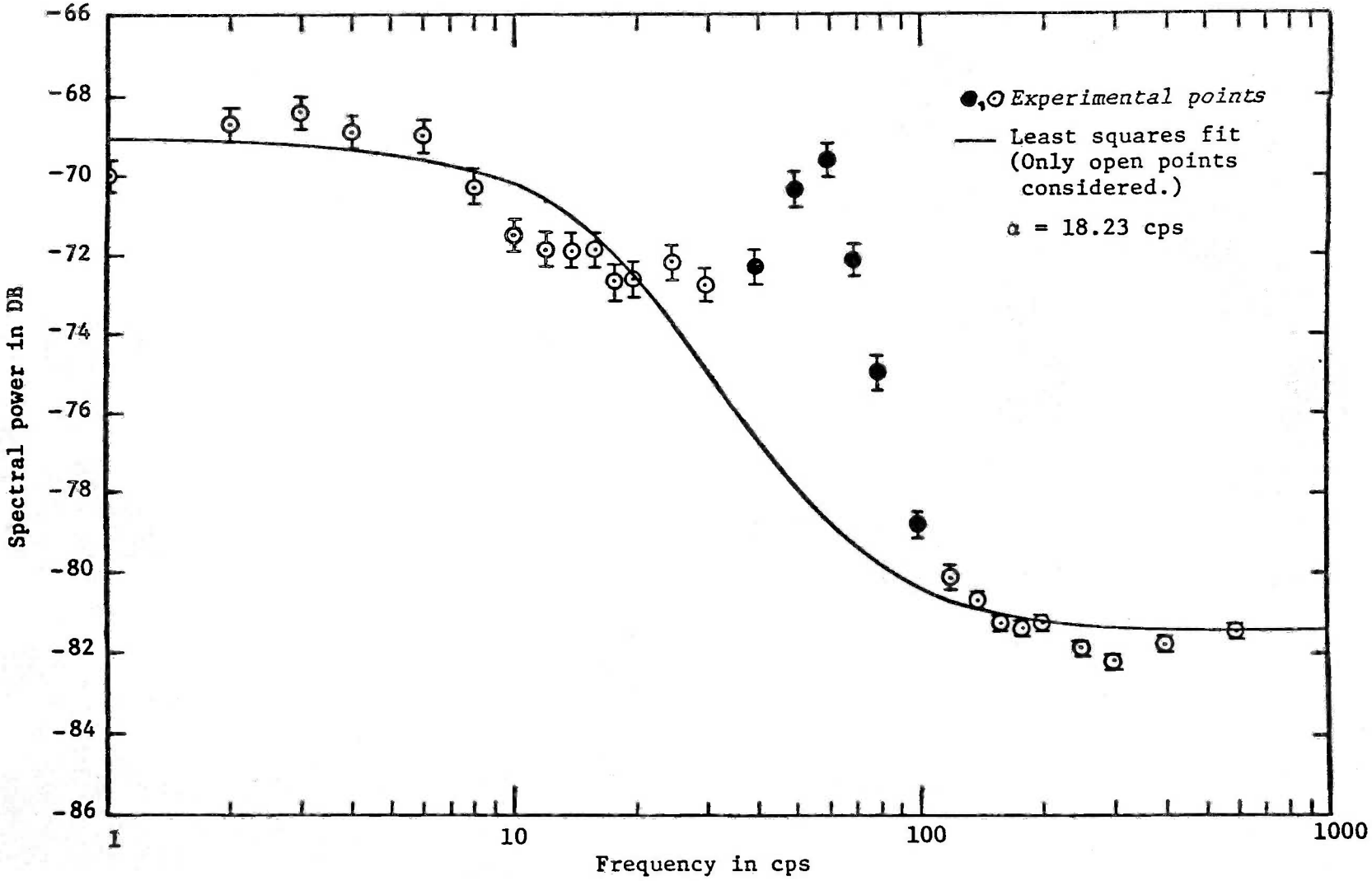

Figure 13. Spectral power at 10 watts.

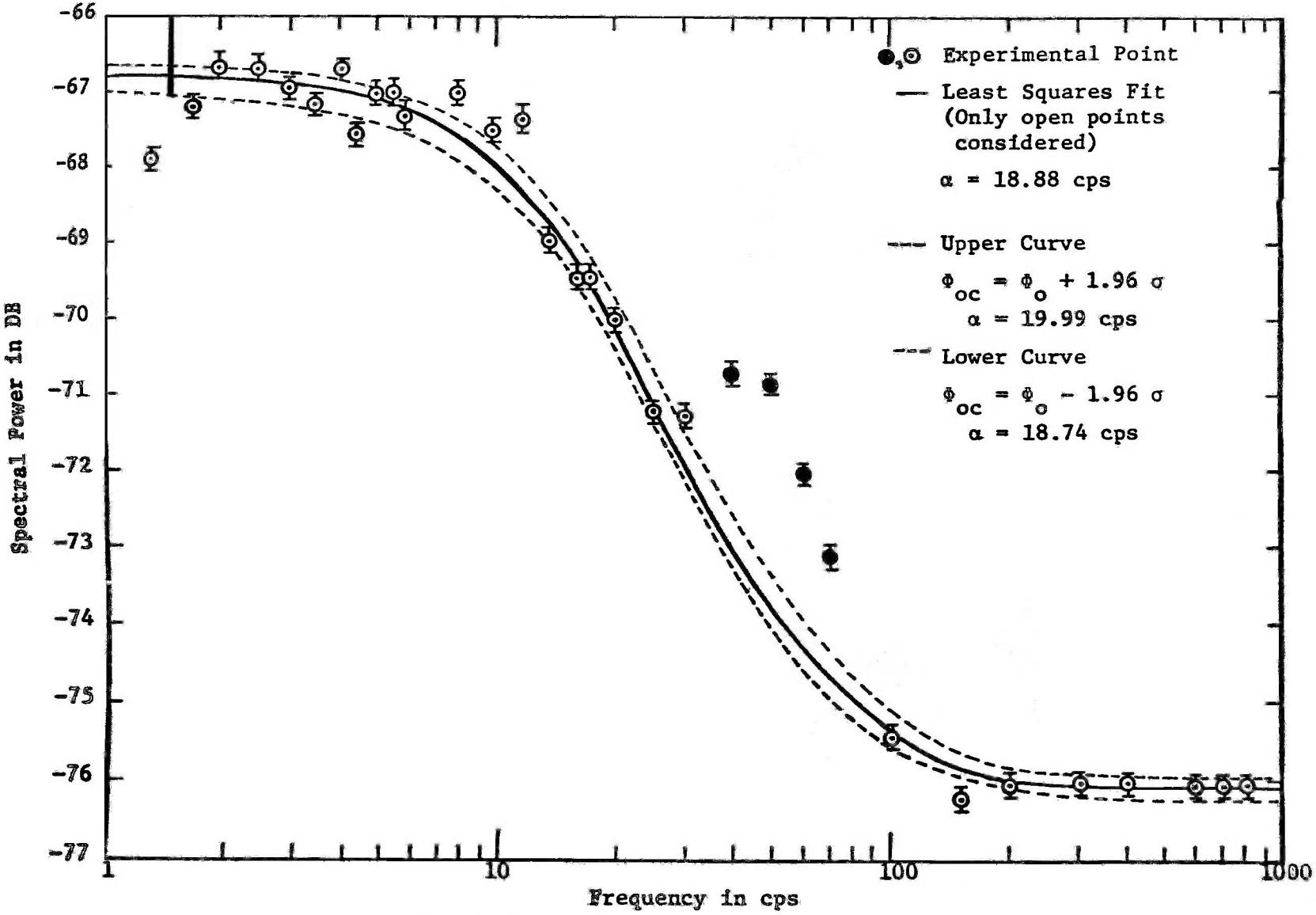

Figure 14. Spectral power at 15 watts.

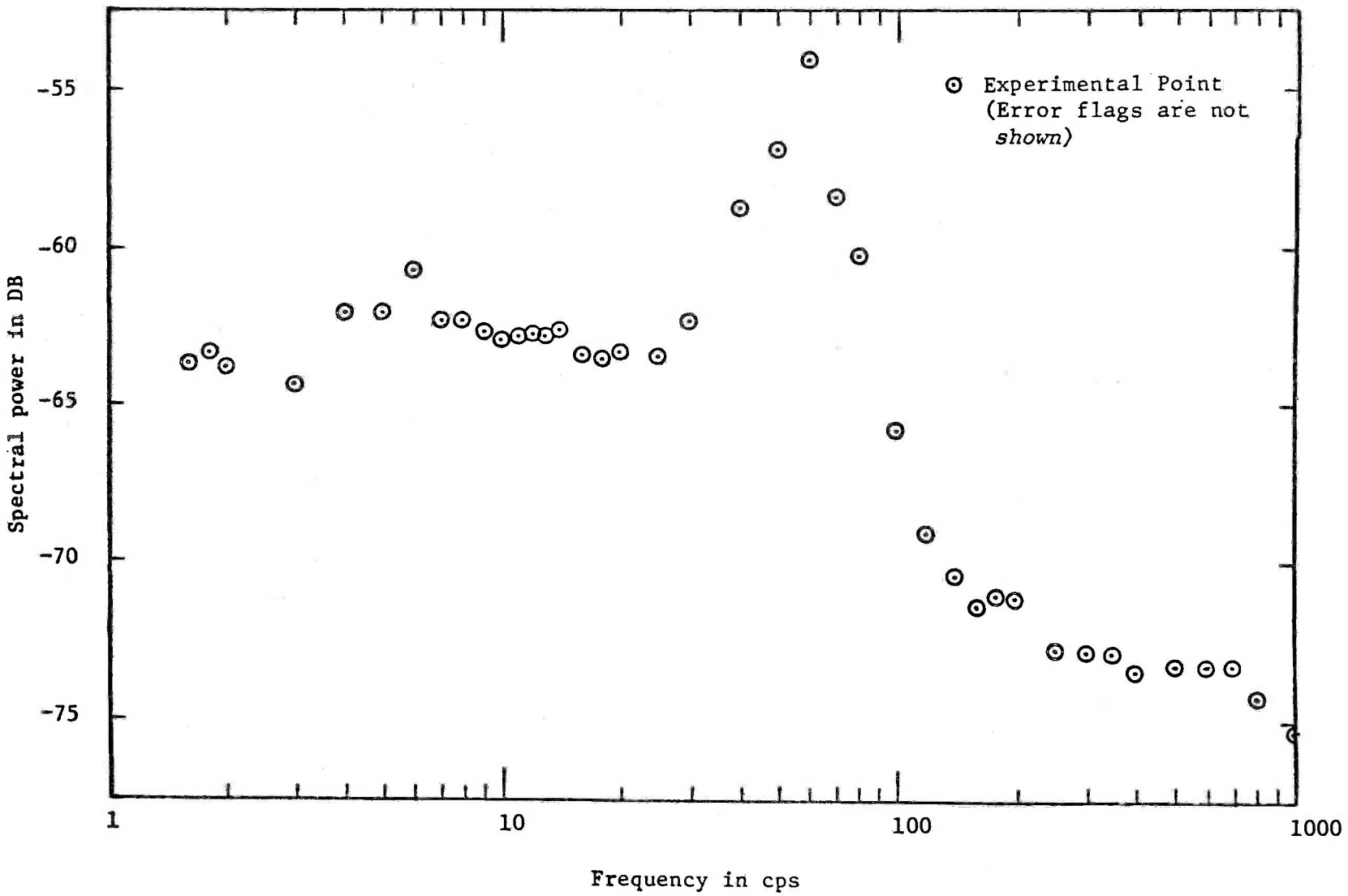

Figure 15. Spectral power at 50 watts.

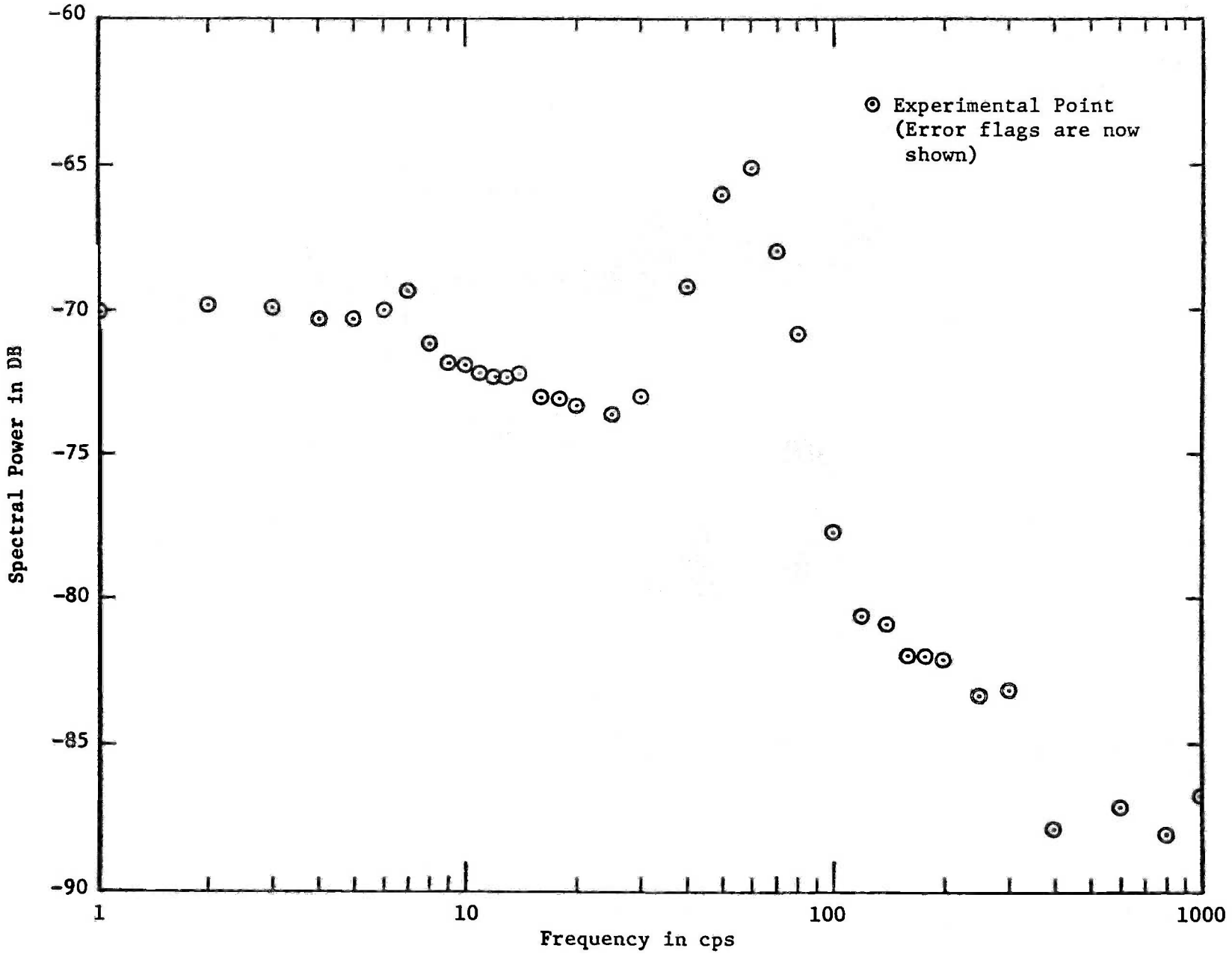

Figure 16. Spectral Power at 100 Watts.

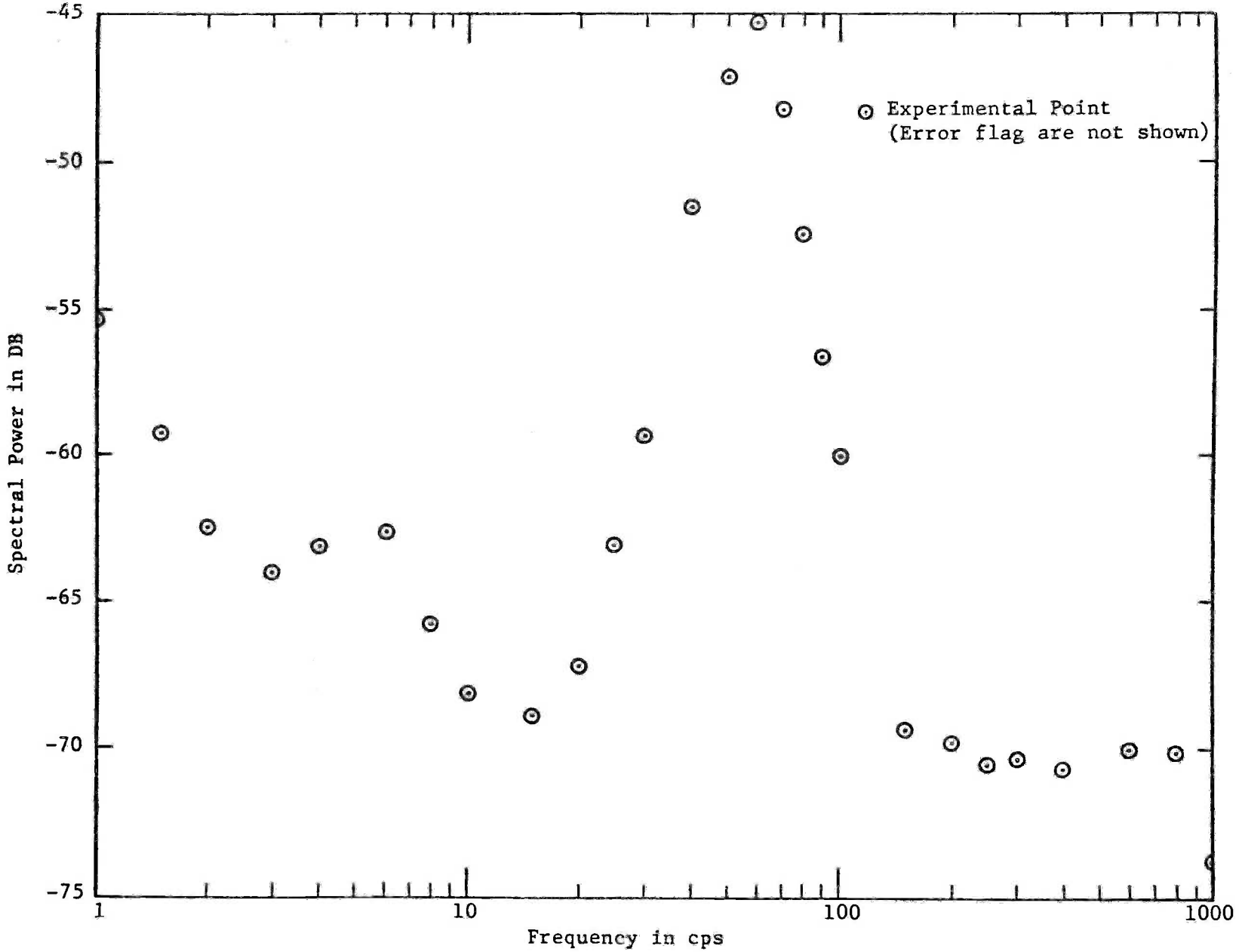

Figure 17. Spectral Power at 70 Kilowatts.

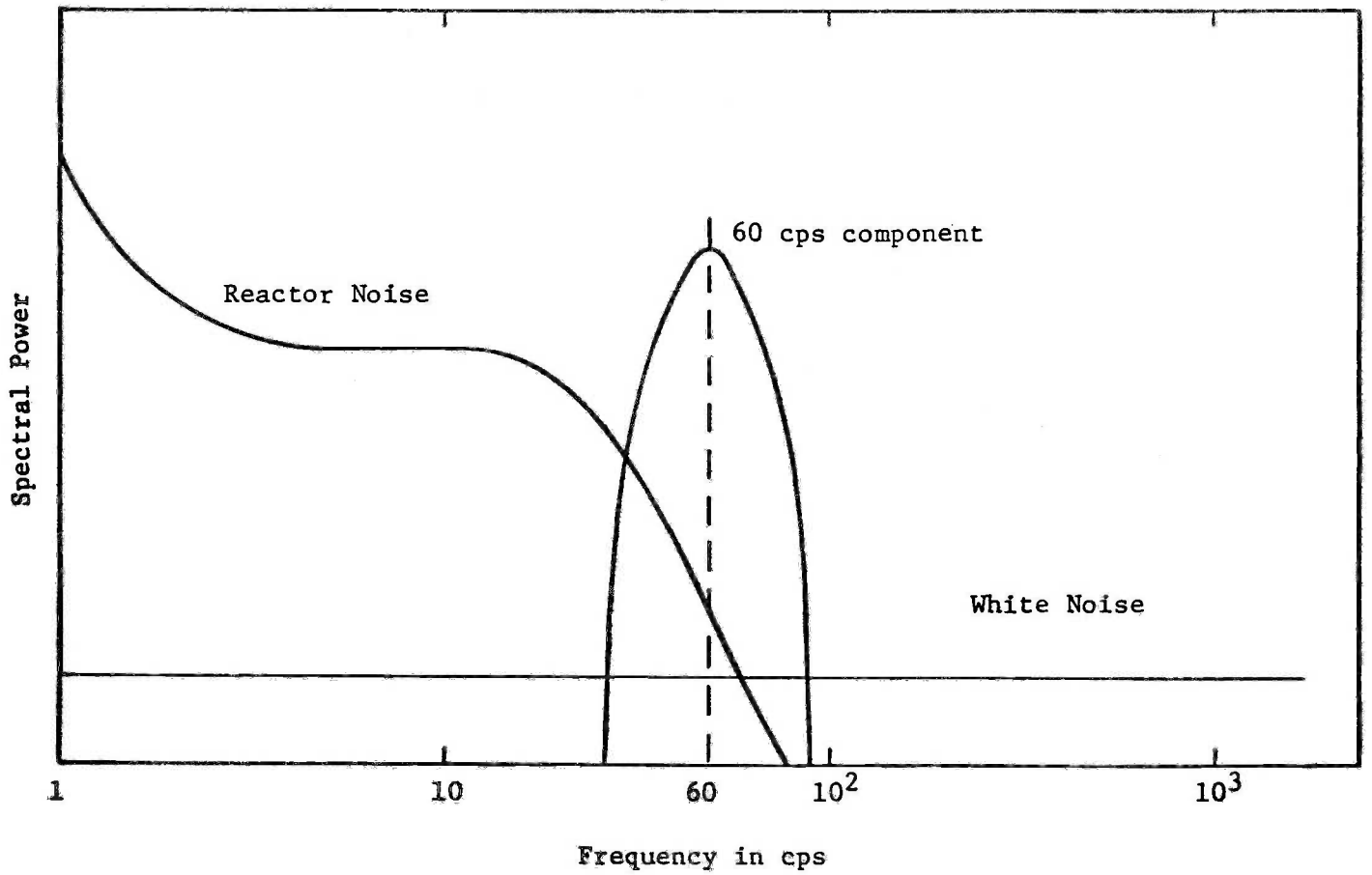

Figure 18. Components of Measured Spectrum.

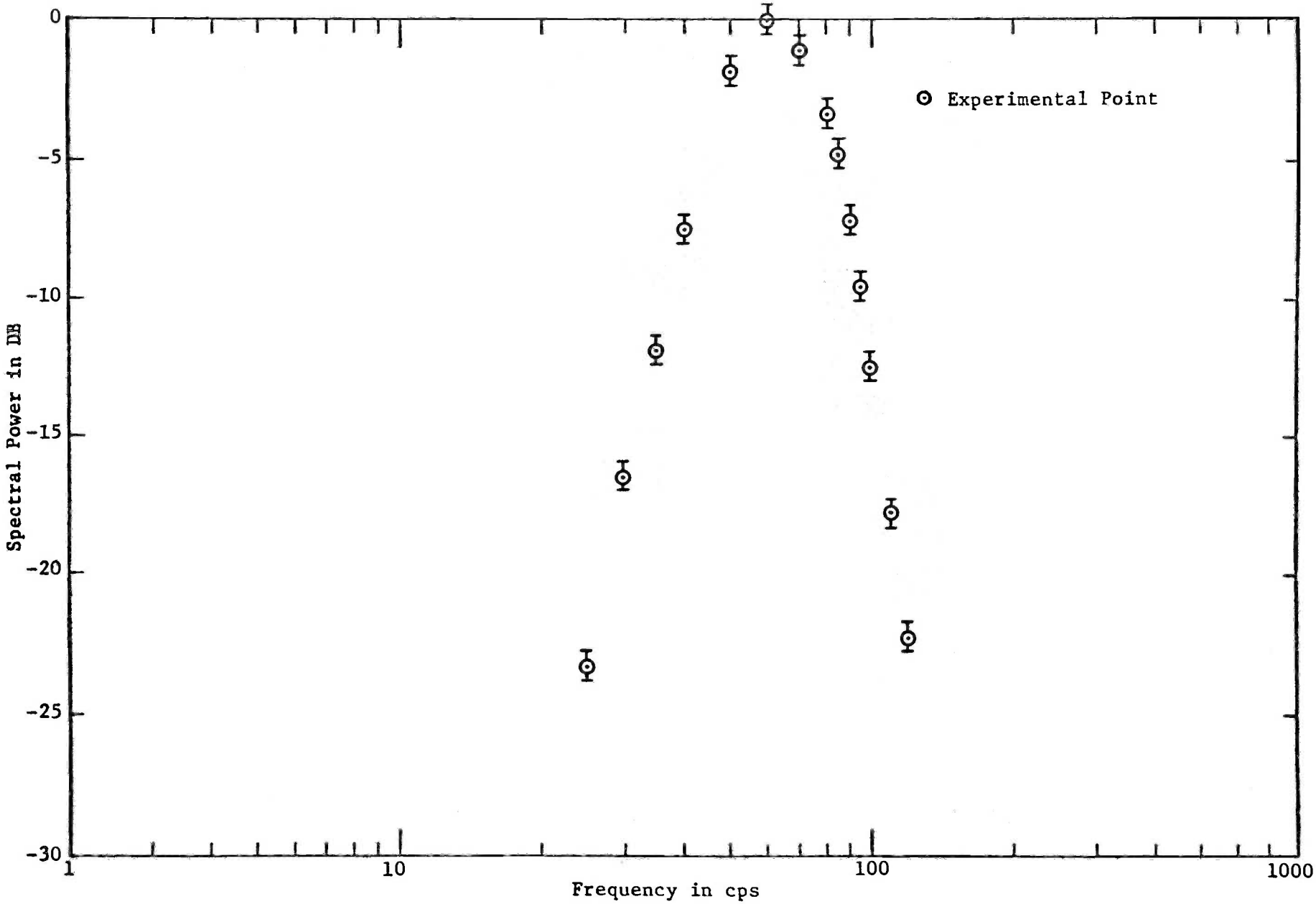

Figure 19. Filter Window.

the filter window shape from the measured spectrum by use of

$$\Phi_c(f) = \Phi_o(f) - k\, W(f) \tag{49}$$

where $\Phi_c(f)$ is the corrected spectral power, Φ_o is the measured spectral power, k an arbitrary constant, less than 1, and W(f) the filter window shape. The numerical calculations were done on the IBM-1410 digital computer for several values of k. Appendix E describes the computer code used. Each resulting set of data was then fit to a function of the form

$$\Phi(f) = A + \frac{B}{\alpha^2 + \omega^2} \tag{50}$$

by a least squares technique, in which the least squares error was calculated from

$$E_i^2 = \left[\frac{\Phi_c(f_i) - \Phi_o(f_i)}{\Phi_o(f_i)} \right]^2 . \tag{51}$$

The errors were weighted with a $F(f)^{-1}$ factor so that all points would have equal importance, as the range of values for $\Phi_o(f)$ spanned over three decades. The set of data which had the smallest E_i^2 was assumed to have the proper value of k.

Figure 12 shows the corrected points obtained by this analytical reduction. The reduction required a large amount of computer time, as the proper value of the constant k had to be selected by trial and error. It was attempted in case 17 (power level 10 watts) with no satisfactory results. A more refined determination of k would yield an improvement in the results. The removal of the peak was not done in the other cases, as the frequencies

where it appears are not of importance for the evaluation of either the break frequency or for the power calibration. This 60 cps peak was observed in the results of similar work done by other researchers (40).

An examination of Figures 13 through 17 shows a deterioration of the reactor transfer function as the power increases. This is due to the fact that at higher powers the temperature feedback effect takes place.

As indicated before, if it is desired to obtain a certain error in the experimental data, the reactor noise must be analyzed for a minimum length of time, and, consequently, the reactor must be operated at a steady power level for such a time. In this work that time was chosen to be 20 minutes. In the course of the experimental work it was found that the power level drifted during that length of time. This instability increased with the power level. At low power levels it was possible to obtain sets of good data, with the power level shifting within reasonable limits. At higher powers, over 15 watts, it was necessary to move the control rod after the reactor was in operation for 5 or 8 minutes.

The perturbation introduced by the control rod motion in the data is illustrated in Figures 20 and 21. Figure 20 is the output of the analog computer integrating circuit, with the filter set at 3 cps, and Figure 21 with the filter set at 30 cps. Both analyses were done with the same piece of tape.

Several ways were devised to obviate this problem, such as stopping recording before rod motion, but without success. Finally it was decided not to attempt power calibration at high powers. At low power, data acquisition was done without rod motion. The quality of the acquisition was decided by reading the current indicated by the micro-micro-ammeter at regular intervals

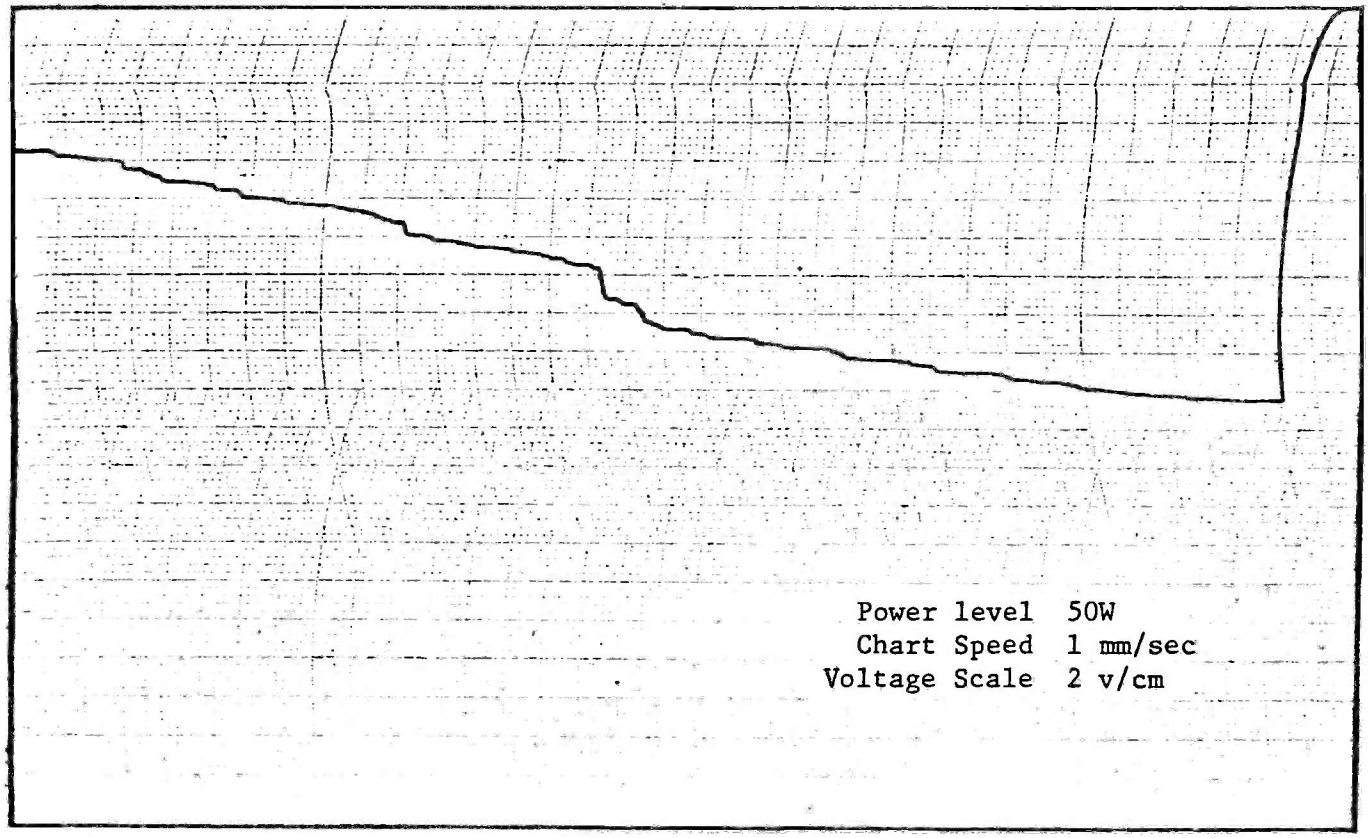

Figure 20. Effect of control rod motion at 3 cps.

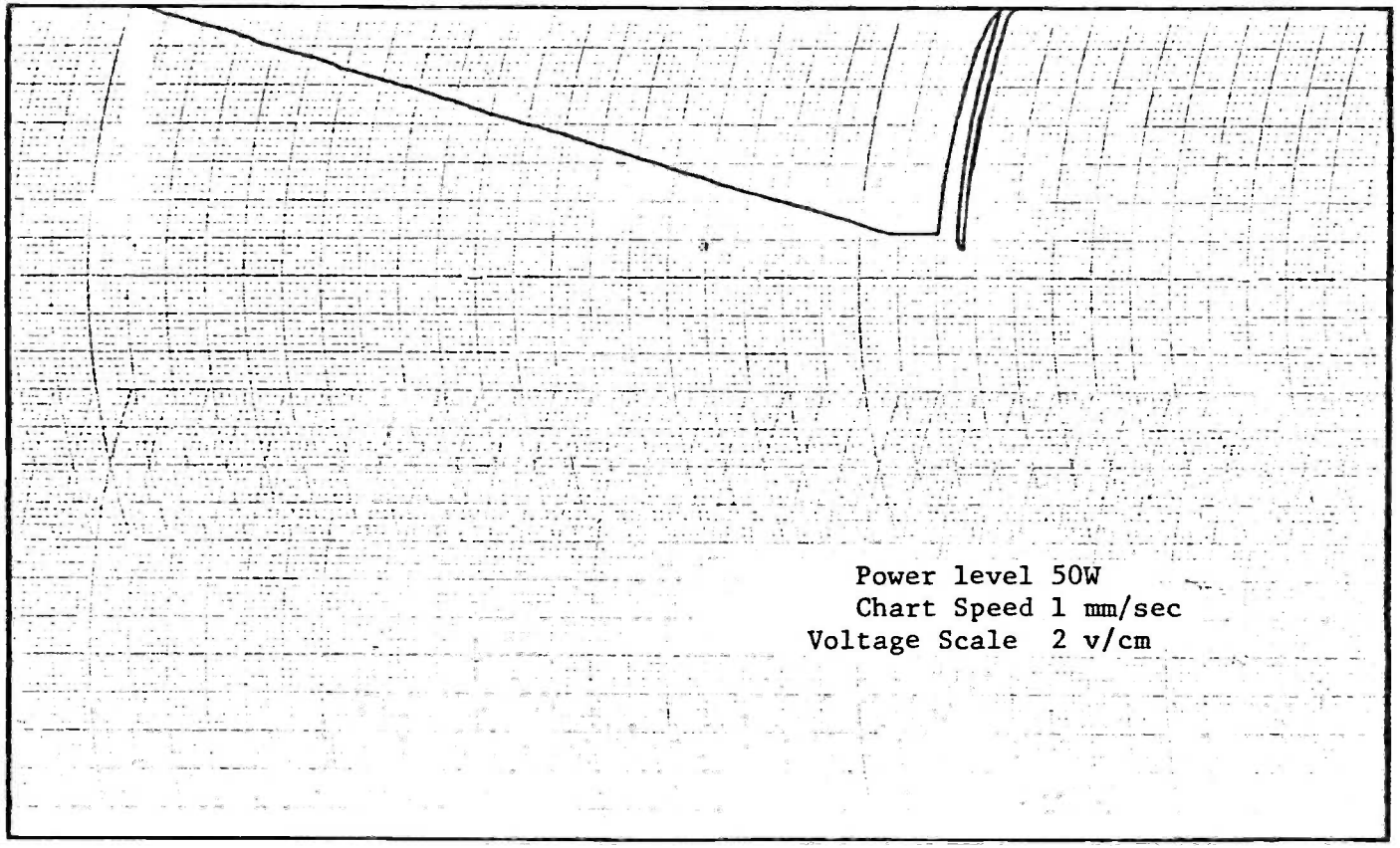

Figure 21. Effect of control rod motion at 30 cps.

and by post-examination of control console records. At power levels of 1, 10, and 15 watts it was possible to obtain a minimum of 20 minutes of good data with power shifts within reasonable limits.

Another problem was encountered during data analysis. The integration time increased with decreasing frequencies. At 1 cps it is 1250 seconds. For integration times over 3 minutes the analog computer integrating circuit becomes unstable. This was overcome by recording at low speed and playing back at high speed. The results tend to confirm this procedure. The data points on Figure 13 were recorded and played back at the same speed. Those of Figure 14 were recorded at 1-7/8 ips and played back at 30 ips; substantial improvement was obtained, but results were not quite satisfactory and the need for a higher speed multiplication was apparent. This set of limitations put a lower limit to the frequency which could be analyzed. On some similar works on noise analysis (40), the playback speed was 1024 times the recording speed, which permitted analysis of frequencies below 2 cps.

It can be observed in Figures 12, 13 and 14 that the spectral power decreases at frequencies below 2 cps. Theory predicts that it should remain constant and then increase at the frequency corresponding to the smallest value of λ_i. This frequency for the KSUTMII reactor is 0.48 cps (35). A similar decrease in the spectral power is noted in the works of Cohn (8) and Yamada (44) and was reported by several other researchers (40). The reason for this deviation probably lies in the fact that the small shifts in power have a greater significance in the power spectrum at low frequencies from 1 to 10 cps, than at frequencies greater than 10 cps. It may be also due to analog computer drifts, because the integration time becomes greater at frequencies below 10 cps. But the possibility is open that some in-core phenomena are responsible.

The standard deviation, σ, associated with the statistical nature of particular calculated spectral estimates at some frequency f has been shown to be (5), (23) and (40)

$$\sigma = \frac{\Phi_o}{\sqrt{t \cdot \Delta f}} \tag{52}$$

where Φ_o is the spectral power, t is the integrating time and Δf is the spectral window, which is related to the frequency by

$$\Delta f = 0.53\ f\ . \tag{53}$$

The break frequency, α, was calculated by a least squares fit of the experimental points to a function of the form

$$\Phi_o = A + \frac{B}{\alpha^2 + \omega^2}\ . \tag{54}$$

By differentiation with respect to α, A and B a set of three normal equations was obtained (Appendix C). An iterative technique based on the Newton-Raphson method was used to solve for α. The numerical calculations were done on the IBM-1410 computer. Appendix F outlines the iteration technique used and describes the computer code.

The break frequency was calculated for cases 8, 17 and 23 (power levels of 1, 10 and 15 watts respectively). The results are presented in Table IV. An error analysis on the value of α is difficult to perform. The problem arises from the non-linearity of Eqs. (C-1), (C-2), and (C-3), and the convergence of the iterative technique. It was decided to set confidence bands to the experimental points. This approach is in line with other experimenters' approaches. It has been used, among others, by Cohn (8) to

determine the break frequency of the ZPR-III and ZPR-V reactors. Several other cases are reported in reference (40). The theoretical development of this approach is extensively treated in (5), (13), (23) and (40).

Table IV. Calculated Break Frequency

Case No.	Power Level in Watts	Break Frequency in radians/second	Break Frequency in cps
8	1	122.30	19.46
17	10	114.55	18.23
23	15	118.62	18.88

The standard deviations of the experimental points, obtained from Eq. (52), were multiplied by 1.96 and sets of new points were obtained from

$$\Phi_{oc} = \Phi_o \pm 1.96\ \sigma \qquad (55)$$

where Φ_o are the experimentally calculated spectral points and Φ_{oc} the corrected spectral points.

These new sets of spectral points were fit to the theoretical curve by a least squares technique and upper and lower bands were obtained. These bands were solved for α, and upper and lower values of α were obtained.

This approach was used in case 23 (power level of 15 watts). The upper and lower bands are indicated in Figure 14. The upper value for α was 19.99 cps and the lower 18.73 cps.

With the values for β and ℓ^* given in (35), the theoretical break frequency for the KSUTMII reactor is 19.36 cps. The break frequency of the

KSUTMII reactor was experimentally determined previously by rod oscillation techniques (3) and by autocorrelation methods (27). The values obtained are tabulated in Table V.

Table V. KSUTMII Reactor Break Frequency Obtained by Different Methods

Method		Break Frequency in cps
Theoretical	(35)	19.35
Rod Oscillation	(3)	17.9 $\pm$ 0.4
Autocorrelation	(27)	18.5 $\pm$ 0.1
Noise Analysis	(this work)	19.3 $\pm$ 0.6

The calibration curve for the analyzing circuit is presented in Figure 22.

The detector efficiency, ε, and the charge transferred per neutron absorbed were calculated from formulas (17) and (18) respectively. The reactor power level was calculated from formula (30). Table VI summarizes these results.

The values of ε are in the same order of magnitude as the value reported by Scröder (32) who determined $\varepsilon = 0.0012$ with an estimated error of less than 10%. The difference in values is accounted for by differences in detector characteristics. The value of Q also compares favorably with the values of 3.9×10^{-15} and 2.62×10^{-15} reported by other authors (32)(44).

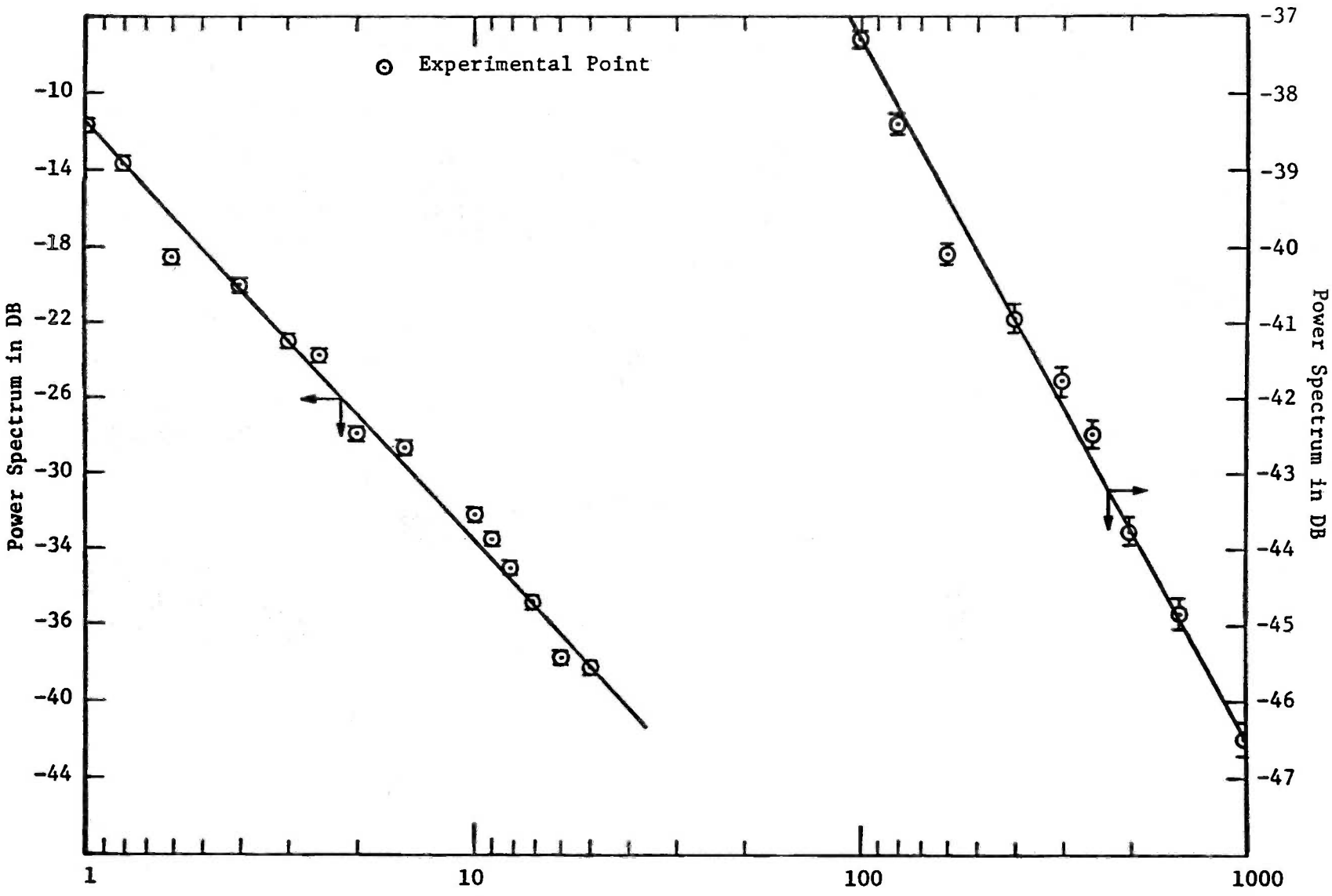

Figure 22. Calibration Curve for Data Analysis Circuit.

Table VI. Summary of Results

Case No.	Console Power Level in Watts	$\bar{I}$ in amps	ε	Q in Coulombs	Calculated Power in Watts
8	1	$(2.76 \pm .08) \times 10^{-7}$	0.042 ± 0.004	$(3.95 \pm .12) \times 10^{-16}$	$0.54 \pm .02$
17	10	$(2.20 \pm .06) \times 10^{-6}$	0.036 ± 0.004	$(1.68 \pm .05) \times 10^{-16}$	$11.54 \pm .50$
23	15	$(3.50 \pm .07) \times 10^{-6}$	0.042 ± 0.004	$(1.42 \pm .04) \times 10^{-16}$	$18.72 \pm .81$

It is observed from Table VI that the values of ε and Q change with power. This may be due to two facts: first, that the chamber efficiency is a function of the neutron population; second, that there is not precise assurance that the detector was placed at the same elevation within the core in each case. Each experiment was conducted on different days. The position of the detector is irrelevant for the determination of the transfer function, evaluation of the break frequency and power calibration, provided it remains at the same place during the length of data acquisition and is placed at a point where the reactor noise is greater than the instrument noise.

Study of the variation of $\bar{I}$ with power tends to indicate a non-linear dependence. This may be accounted for by changes in detector position from case to case. Nevertheless an experiment was conducted in which the detector was kept at the same position while the reactor power was increased to different levels. The results of this experiment are presented in tabulated form on the following page.

Table VII. Dependence of Average Current Through Detector with Power Level

Console Power Level in Watts	$\bar{I}$ in amps
1	4.66×10^{-8}
15	6.90×10^{-7}
25	1.13×10^{-6}
100	4.45×10^{-6}
500	2.35×10^{-5}
1×10^{3}	4.45×10^{-5}
1×10^{4}	2.65×10^{-4}

These results indicate a linear dependence up to powers of 1 kw, but not above.

The results for the calculated power indicate a discrepancy with the power indicated by the linear recorder of the reactor console. This discrepancy increases with power. For the power levels of 50 and 100 watts, it can be explained by the temperature feedback effects, which begin to have an effect on the transfer function as the power level increases.

The reactor power is a function of three variables, i.e., $\bar{I}$, ε and Q, Eq. (30). By multiplication of Eqs. (17) and (18), one obtains

$$Q \times \varepsilon = \frac{\beta^2}{\frac{\bar{\nu}^2 - \bar{\nu}}{\bar{\nu}^2}} \left\{ \langle |I(1)|^2 \rangle - \langle |I(\infty)|^2 \rangle \right\} . \qquad (56)$$

The first factor in the expression between brackets was found to be, in the course of this work, of the order of 10 times greater than $<|I(\infty)|^2>$. Consequently the calculated reactor power chiefly depends on $<|I(1)|^2>$, the spectral power at a frequency range between 2 cps and 10 cps. It was previously explained that the spectral power at low frequencies was difficult to obtain with accuracy due to a variety of circumstances.

All calculated powers, case 8 excepted, are higher than the power indicated by the linear recorder of the reactor console. This fact indicates that the calculated values for $<|I(1)|^2>$ are smaller than the true ones. It was indicated before that the spectral power decreases at frequencies below 2 cps, where theory predicts it should remain constant. This was attributed to a greater significance of power drifts at low frequencies and to analog computer drifts. Apparently the effects of these phenomena extended to frequencies greater than 2 cps.

The calculated power for case 8 was obtained from the results of a graduate laboratory (19) and did not include all the refinements in analysis which were later found to be necessary such as tape speed multiplication. In addition it is likely that instrument noise may have become significant at this low power and caused some distortion of the power spectrum.

Rather than refer to the reactor power level it is more appropriate to refer to the average reactor power during the length of data acquisition, the reason being that the reactor power shifted slightly during that time. Examination of the linear recorder trace on the reactor console indicated little or no deviation in cases 8 and 17. However, the trace for case 23 indicated a steady drift from 15 to 16.2 watts during the time of data

acquisition. Thus the average power during the recording of data for case 23 was 15.6 watts.

Further indication of the errors encountered in this work were given by comparison of the calculated powers indicated by the linear recorder of the reactor console, presented in tabulated form below.

Table VIII. Comparisons of Results

Case No. *	Nominal Console Power Level in Watts	Average Nominal Console Power Level in Watts	Calculated Power in Watts	Discrepancy
8	1	1	0.54 ± 0.02	46.0
17	10	10	11.54 ± 0.50	15.4
23	15	15.6	18.72 ± 0.81	20.0

The apparent contradiction between the good results reported for the break frequency and the results for the calculated power level results from the fact that the frequency range of interest to calculate the break frequency lies between 10 cps and 30 cps, where no significant problems were encountered during the analysis of data. However, the range of interest for the calculation of power lies below 10 cps, where, as explained previously, inherent errors in this method caused difficulty in the analysis.

* Dates and times of runs:

Case 8: December 14, 1966, at 9:45 a.m.

Case 17: June 6, 1967, at 2:00 p.m.

Case 23: July 6, 1967, at 4:15 p.m.

6.0 CONCLUSIONS

The results of these investigations have led to several conclusions as stated below:

1. The determination of the zero power reactor transfer function by noise analysis is possible, although it involves a considerable amount of effort.
2. The low frequency part of the transfer function is difficult to obtain with precision. The use of multiple speed tape recorders simplifies data analysis. The method is evidently very sensitive to the sophistication of equipment in use.
3. The use of specially designed electronic analyzers (8), which perform functions of amplification, filtering, detection and recording, could lead to better results and less cumbersome data acquisition and analysis.
4. The determination of the zero-power transfer function by noise analysis is less informative than obtained by rod oscillation techniques, because no phase information is obtained unless autocorrelation techniques are used.
5. The determination of the break frequency in this research leads to results comparable to results obtained by other techniques. As the frequencies of interest in determining the break frequency lie from about 10 cps to 30 cps, most of the problems encountered in this work are avoided.
6. The determination of the reactor power by noise analysis seems rather cumbersome and probably of no immediate

application to power reactors. The inherent errors are of importance due to the lack of accuracy in the determination of the power spectrum at low frequencies. In this work, approximately 10 hours are required to calculate a power level.

8. Noise analysis techniques do not require special in-core instrumentation and do not interfere with the normal operation of the reactor. They seem rather appropriate to stability studies of power reactors.

7.0 SUGGESTIONS FOR FURTHER STUDIES

The field of noise analysis offers a wide scope for investigation in reactor dynamics. To indicate two, noise analysis may be applied to obtain delayed neutron parameters (39), and measurements in subcritical reactors (38).

The KSUTMII reactor break frequency has been obtained by two different methods (3)(46), besides the method reported in this work. Another method is available. This method is usually known as the Rossi-alpha experiment and essentially consists of studying the time behavior of neutrons having a single common ancestor (15). This experiment, if done at the KSUTMII reactor, could yield a more accurate value of the break frequency.

The use of a tape recorder with a speed ratio of the order of 1,000 or over would permit the determination of the spectral power for frequencies below 2 cps, and would allow the calculation of the delayed neutron parameters.

As pointed out before, the use of autocorrelation techniques would give phase information of the zero-power transfer function.

A digital approach to noise analysis techniques on the TRIGA Mark II reactor can be made. Whether a digital or continuous analysis is more appropriate depends on a variety of factors. In general, digital analysis requires more expensive equipment and the digital computer time could be extensive.

8.0 ACKNOWLEDGMENTS

The author wishes to express his gratitude and appreciation to Dr. W. R. Kimel, Head of the Kansas State University Department of Nuclear Engineering for his encouragement, help and guidance, and to Dr. M. Copic, Visiting Professor from Josef Stefan Nuclear Institute, Ljubljana, Yugoslavia, for his criticism and suggestions. Thanks are also due to Professor R. W. Clack and Mr. R. E. Hightower. Special thanks are due to Mr. R. E. Kaiser for his helpful cooperation and advice during all phases of this work. Thanks are extended to the Kansas State University Engineering Experiment Station and to Tecnatom S.A., Madrid, Spain for their financial support.

9.0 LITERATURE CITED

1. Albrecht, R. W., A System for Reactor Noise Measurement, Proceedings of a Symposium held at the University of Arizona, 1963.

2. Albrecht, R. W., Measurements of Dynamics Nuclear Reactor Parameters by Methods of Stochastic Process, Trans. Amer. Nucl. Soc. 4, 2:311 (1961).

3. Beeson, C. L., Measurement of the Zero Power Transfer Function of the Kansas State University TRIGA Mark II Nuclear Reactor, Master's Thesis, Kansas State University, Manhattan, Kansas, 1966.

4. Bennett, E. F., The Rice Formulation of Pile Noise, Nucl. Sci. and Eng., 8, 53 (1960).

5. Blackman, R. B. and J. W. Tukey, The Measurement of Noise Spectra, Dover Publications, Inc., New York (1958).

6. Brunson, G. S., et al., Measuring the Prompt Period of a Reactor, Nucleonics 15, 11:132 (1957).

7. Carslaw, H. S., Introduction to the Theory of Fourier Series and Integrals, 3rd Ed., MacMillan and Sons, London (1930).

8. Cohn, C. H., Determination of Reactor Kinetics Parameter by Pile Noise Analysis, Nucl. Sci. and Eng., 5:331 (1959).

9. Cohn, C. H., A Simplified Theory of Pile Noise, Nucl. Sci. and Eng., 7, 472 (1960).

10. Courant, E. D. and P. R. Wallace, Fluctuations in the Number of Neutrons in a Pile, Phys. Rev. 72, 1038 (1947).

11. Cummings, J. D., Frequency Spectrum of Calder Hall Reactor Noise, A.E.E.W.-M-19, Jan., 1960.

12. deHoffman, F., Intensity Fluctuations of a Neutron Chain Reactor, MDDC-382 (1946).

13. Deming, W. E., Statistical Adjustment of Data, pp. 167-168, John Wiley and Sons, New York (1943).

14. Diven, B. C., et al., Multiplication of Fission Neutrons, Phys. Rev. 101, 1012 (1956).

15. Feyman, R. F., F. deHoffman and R. Serber, Dispersion of Neutron Emission in U-235, J. Nucl. Energy, 3, 64 (1956).

16. Freeman, J. J., Principles of Noise, John Wiley & Sons, New York (1958).

17. Frisch, O. R. and J. D. Littler, Pile Modulation and Statistical Fluctuations in Pile, Phil. Mag. 45, 126 (1954).

18. Goldman, S., Frequency Analysis, Modulation and Noise, pp. 355-356, McGraw-Hill, Inc., New York (1948).

19. Kaiser, R. E., Personal Communication, Department of Nuclear Engineering, Kansas State University, Manhattan, Kansas (1967).

20. Lapidus, L., Digital Computations for Chemical Engineers, pp. 282-296, McGraw-Hill Book Co., New York (1962).

21. Lawrence, L. A. J. and E. R. Carran, A Record Replay System for the Harmonic Analysis of Nuclear Reactor Flux Noise, A.E.E.W.-M-33, Feb., 1960.

22. Leachman, R. B., Emission of Prompt Neutrons from Fission, Phys. Rev. 101, 1005 (1956).

23. Lee, Y. M., Statistical Theory of Communications, John Wiley & Sons New York (1960).

24. Moore, M. N., The Power Noise Transfer Function of a Reactor, Nucl. Sci. and Eng., 6, 448 (1959).

25. Moore, M. N., The Determination of the Reactor Transfer Function From Measurements at Steady State Operation, Nucl. Sci. and Eng., 3, 387 (1958).

26. Moore, M. N., Reactor Tranfer Functions, Addendum, Nucl. Sci. and Eng., 4, 134 (1958).

27. Nuclear Engineering Laboratory, Students' Results, Department of Nuclear Engineering, Kansas State University, Manhattan, Kansas, 1966.

28. Orndoff, J. D., Prompt Neutron Periods of Metal Cricical Assemblies, Nucl. Sci. and Eng., 2, 450 (1957).

29. Parkinson, T. F., Measurements of the Transfer Function of the University of Florida Training Reactor, Research Reactor Journal 3, 3 (1963).

30. Rice, S. O., Mathematical Analysis of Random Noise, Bell-System Tech. J., 23, 282 (1944) and 24, 46 (1944).

31. Schottky, W., Ann. Physick, 57, 541-567 (1918).

32. Schroder, V. R., Bestimmung der Reaktorleistung mit Hilfe der Reaktorrauschens, Nucleonik 4, 5 (1962).

33. Schultz, M. A., Control of Nuclear Reactor and Power Plants, McGraw-Hill Book Co., New York (1961).

34. Solodovnikov, V. V., Introduction to the Statistical Dynamics of Automatic Control Systems, Dover Publications, Inc., New York (1960).

35. Technical Foundations of TRIGA, General Atomic Report GA-471, pp. 96, (1958).

36. Terrell, J., Distribution of Fission Neutron Numbers, Phys. Rev., 108, 3 (1957).

37. Thie, J. A., Elementary Methods of Reactor Noise Analysis, Nucl. Sci. and Eng., 15, 109 (1963).

38. Thie, J. A., Statistical Analysis of Power Reactor Noise, Nucleonics, 17, 10, 102 (1959).

39. Thie, J. A., Operating Information from Noise Analysis, Nucleonics, 21, 3 (1963).

40. Thie, J. A., Reactor Noise, Rowman and Littlefield, New York (1963).

41. TRIGA Mark II Reactor, General Specifications and Description, General Atomic, Report GA-2627 (Rev.) (1964).

42. Van der Zile, A., Noise, Prentice-Hall, New York (1954).

43. Wax, N., Selected Papers on Noise and Stochastic Processes, Dover Publications, Inc., New York (1954).

44. Yamada, S., Reactor Noise Analysis of Swimming Pool Type Reactors, J. Nucl. Sci. and Tech., 1, 4, 130 (1964).

45. Yule, G. U. and M. G. Kendall, An Introduction to the Theory of Statistics, Hafner Publishing Co., New York (1950).

10.0 APPENDICES

APPENDIX A

Derivation of the Spectral Density of the Noise Equivalent Source (9)

All types of reactions which occur in a reactor and contribute to the noise equivalent source may be classified in two groups:

a) Non-productive absorption, including leakage

b) Fission giving rise to N prompt neutrons.

Let A be the macroscopic cross section for all non-productive neutron absorptions, including leakage, F the macroscopic cross section for fission, n' the number of neutrons in the reactor and ℓ^*, the prompt neutron lifetime. Thus the probability of occurrence of reactions of the first type is $\frac{A}{A+F}$ and the rate of occurrence is $\frac{n'}{\ell^*}\frac{A}{A+F}$. The net number of neutrons produced in reactions of type a) is -1, as a neutron is lost in the process.

In reactions of the second type the probability of occurrence is $\frac{F}{A+F}P_N$, defining P_N as the probability that N prompt neutrons will be produced in any one fission. The average rate of occurrence of reactions of this type is $\frac{n'}{\ell^*}\frac{F}{A+F}P_N$ and the net number of neutrons produced in N-1. These results are summarized in Table A-1.

Let $\bar{\nu}$ be the average number of neutrons produced per one fission. The average rate of fission is $\bar{\nu}\frac{F}{A+F}$. If the reactor is just critical

$$\bar{\nu}\frac{F}{A+F} = 1 . \qquad \text{(A-1)}$$

The probability that N prompt neutrons will be produced in any one fission is subject to the restraints:

$$\sum_{N=1}^{\infty} P_N = 1 \qquad \text{(A-2)}$$

TABLE A-1

Contribution to Pile Noise Source

Nature of Process	Average Rate of Occurrence	Net number of Neutrons Produced
Non-productive absorption including leakage	$\frac{n'}{\ell^*} \cdot \frac{A}{A+F}$	-1
Fission giving rise to N prompt neutrons	$\frac{n'}{\ell^*} \cdot \frac{F}{A+F} \cdot P_{\tilde{N}}$	N-1

and

$$\sum_{N=1}^{\infty} N P_N = (1 - \beta) \bar{\nu} \simeq \bar{\nu} \qquad (A-3)$$

as $\sum_{N=1}^{N} N P_N$ is the number of prompt neutrons produced in any one fission and β is small compared to unity.

Substitution of the quantities in Table A-1 into Eq. (2) yields

$$\langle |S_o(f)|^2 \rangle = \frac{2n'}{\ell^*(A+F)} [A+F \sum_{N=1}^{\infty} (N-1)^2 P_N]. \qquad (A-4)$$

It is pertinent to note that fission processes which produce different numbers of neutrons must be considered to be distinct types of events.

By simple algebraic operations and considering Eqs. (A-1), (A-2), (A-3) and

$$\overline{\nu^2} \simeq \sum_{N=1}^{\infty} N^2 P_N , \qquad (A-5)$$

it is derived that

$$\langle |S_o(f)|^2 \rangle = \frac{2n'}{\ell^*} \left(\frac{\overline{\nu^2} - \bar{\nu}}{\bar{\nu}}\right). \qquad (A-6)$$

It should be emphasized that n' is the number of neutrons in the reactor after the mechanism of fission has taken place. Consequently, the number of neutrons before fission, n, is given by the relationship,

$$n = \frac{n'}{\bar{\nu}} \qquad (A-7)$$

and Eq. (A-6) becomes

$$\langle |S_o(f)|^2 \rangle = \frac{2n}{\ell^*} \left(\frac{\overline{\nu^2} - \bar{\nu}}{\bar{\nu}^2}\right) . \qquad (A-8)$$

APPENDIX B

Source Transfer Function

The source transfer function relates fluctuations in source strength with resulting fluctuations in reactor power level. Its development starts with the one group kinetic equations.

For a critical reactor, $\Delta K = 0$, the one-group kinetics equation is given by Schultz (33) as follows:

$$\frac{dn}{dt} = -\frac{\beta}{\ell^*} n + \sum_{i=1}^{6} \lambda_i C_i + S(t) \tag{B-1}$$

$$\frac{dC_i}{dt} = \frac{\beta_i}{\ell^*} n - \lambda_i C_i \tag{B-2}$$

where the symbols have their usual meanings.

The neutron population, n, and the delayed neutron precursor population C_i, are considered to be composed of a steady part, n_o, and C_{io}, and a fluctuating part, n(t) and $C_i(t)$, respectively. Thus:

$$n = n_o + n(t) \tag{B-3}$$

$$C_i = C_{io} + C_i(t). \tag{B-4}$$

Since the reactor is critical there is not a steady source. At steady state the following conditions hold:

$$n(t) = 0 \tag{B-5}$$

$$C_i(t) = 0$$

$$S(t) = 0$$

$$\frac{dn(t)}{dt} = 0$$

$$\frac{dC_i(t)}{dt} = 0.$$

Considering Eqs. (B-3), (B-4) and (B-5), Eqs. (B-1) and (B-2) become respectively:

$$\frac{dn(t)}{dt} = -\frac{\beta}{\ell^*} n(t) + \sum_{i=1}^{6} \lambda_i C_i(t) + S(t) \tag{B-6}$$

$$\frac{dC_i(t)}{dt} = \frac{\beta_i}{\ell^*} n(t) - \lambda_i C_i(t). \tag{B-7}$$

In the assumption of a sinusoidal dependence for $n(t)$, $C_i(t)$ and $S(t)$, they can be expressed as:

$$n(t) = n(f)\, e^{i2\pi f} \tag{B-8}$$

$$C_i(t) = C_i(f)\, e^{i2\pi f} \tag{B-9}$$

$$S(t) = S(f)\, e^{i2\pi f}. \tag{B-10}$$

By substitution into Eqs. (B-6) and (B-7) and by elimination of $C_i(f)$ one obtains

$$S(f) = n(f) \left\{ i2\pi f + \frac{\beta}{\ell^*} \sum_{i=1}^{6} \frac{\lambda_i \beta_i}{\ell^*(i2\pi f + \lambda_i)} \right\}. \tag{B-11}$$

It is customary to express the reactor transfer function $T(f)$ as the quotient $n(f)/S(f)$; therefore,

$$T(f) = \frac{n(f)}{S(f)} = \frac{\ell^*}{i2\pi f\ell^* + \beta - \sum_{i=1}^{6} \frac{\lambda_i \beta_i}{i2\pi f + \lambda_i}} . \tag{B-12}$$

Letting

$$L = \ell^* + \sum_{i=1}^{6} \frac{\lambda_i \beta_i}{(2\pi f)^2 + \lambda_i^2} \tag{B-13}$$

and

$$B = \beta - \sum_{i=1}^{6} \frac{\lambda_i \beta_i}{(2\pi f)^2 + \lambda_i^2} \tag{B-14}$$

and considering that $\beta = \sum_{i=1}^{6} \beta_i$, after proper operations on Eq. (B-12) one obtains

$$T(f) = \frac{\ell^*}{2\pi i f L + B} . \tag{B-15}$$

The modulus of the transfer function is given by:

$$|T(f)|^2 = \frac{\ell^{*2}}{(2\pi f L)^2 + B^2} . \tag{B-16}$$

The spectral density of the fluctuations in the reactor neutron population may now be obtained from

$$\langle |n(f)|^2 \rangle = |T(f)|^2 \langle |S_o(f)|^2 \rangle . \tag{B-17}$$

By substitution of the expression for $\langle |S_o|^2 \rangle$ given by Eq. (3), one obtains

$$\langle |n(f)|^2 \rangle = \frac{2n\ell^*}{(2\pi f L)^2 + B^2} \left(\frac{\overline{\nu^2} - \bar{\nu}}{\bar{\nu}^2}\right) . \tag{B-18}$$

APPENDIX C

Least Squares Fit of the Experimental Data

Differentiating Eq. (39), with respect to A, B, and α, respectively, gives the following three normal equations to be solved

$$\frac{\partial S}{\partial A} = 0 = 2 \sum_{i=1}^{N} (y_i - n_i^2) \tag{C-1}$$

$$\frac{\partial S}{\partial B} = 0 = 2 \sum_{i=1}^{N} \left\{(y_i - n_i^2) \frac{1}{\alpha^2 + \omega_i^2}\right\} \tag{C-2}$$

$$\frac{\partial S}{\partial \alpha} = 0 = 2 \sum_{i=1}^{N} \left\{(y_i - n_i^2) \frac{-2\alpha B}{(\alpha^2 + \omega_i^2)^2}\right\} \tag{C-3}$$

where N is the number of data points and $y_i = A + \frac{B}{\alpha^2 + \omega_i^2}$.

Let

$$M = \sum_{i=1}^{N} n_i^2$$

$$P = \sum_{i=1}^{N} \frac{1}{\alpha^2 + \omega_i^2}$$

$$R = \sum_{i=1}^{N} \frac{n_i^2}{\alpha^2 + \omega_i^2}$$

$$T = \sum_{i=1}^{N} \frac{1}{(\alpha^2 + \omega_i^2)^2}$$

$$J = \sum_{i=1}^{N} \frac{n_i^2}{(\alpha^2 + \omega_i^2)^2}$$

$$L = \sum_{i=1}^{N} \frac{1}{(\alpha^2 + \omega_i^2)^3} . \tag{C-4}$$

In this notation Eqs. (C-1), (C-2) and (C-3) become

$$M - NA - PB = 0, \tag{C-5}$$

$$R - AP - TB = 0, \tag{C-6}$$

$$J - TA - LB = 0. \tag{C-7}$$

The first two equations, Eqs. (C-5) and (C-6), are linear in A and B and were solved directly for A and B in terms of α. The last equation, Eq. (C-7), is non-linear; therefore, it cannot be solved directly for α. Elimination of A and B from the first two equations gives

$$A = \frac{RP - MT}{P^2 - NT} \tag{C-8}$$

and

$$B = \frac{PM - RN}{P^2 - NT} \quad . \tag{C-9}$$

An iterative technique based on the Newton-Raphson method was used to solve Eq. (C-7) for α. The details of this iteration method and the description of the IBM-1410 computer program are outlined in Appendix F.

APPENDIX D

Description and Explanation of the IBM-1410 Computer Program Used for Reduction of Data

This computer program calculated the power spectrum by making use of the formula

$$\Phi_0(f) = \frac{V}{t \cdot f \cdot G_A \cdot G_B^2} \qquad \text{(D-1)}$$

where $\Phi_0(f)$ is the power spectrum, V the integrated voltage, t the chart integration time, f the frequency in cps, G_A gain after squaring and G_B the gain before squaring. The output data of this program were the frequency in cps and the power spectrum in decibels.

```
     MON$$     JOB  NOISE ANALYSIS DATA REDUCTION
      DIMENSION T(100),D(100),F(100),GA(100),GB(100),TF(100),TFA(100)
 1000 FORMAT (I6)
 1001 FORMAT(6F12.6)
 2000 FORMAT (1H1,10HINPUT DATA//6X,9HFREQUENCY,9X,4HTIME,9X,7HVOLTAGE,6
     1X,11HGAIN BEFORE,6X,10HGAIN AFTER/)
 2001 FORMAT (1H ,0P3F15.6,1P2E15.5)
 2002 FORMAT (1H1,40X,48HUNNORMALIZED TRANSFER FUNCTION BY NOISE ANALYSI
     1S///11X,14HFREQUENCY, CPS,15X,21HTRANSFER FUNCTION, DB,15X,28HTRAN
     2SFER FUNCTION, ARB UNITS/)
 2004 FORMAT (1H ,13X,0PF10.4,22X,0PF10.4,26X,1PE15.8)
 3000 FORMAT (I6)
 3001 FORMAT (6F12.6)
C         NPT - NUMBER OF DATA POINTS
C         F - FREQUENCY, CPS
C         T - CHART INTEGRATION TIME
C         D - INTEGRATED VOLTAGE
C         GA - GAIN AFTER SQUARING
C         GB - GAIN BEFORE SQUARING
    1 READ (1,1000) NPT
      IF(NPT.EQ.0) CALL EXIT
      DO 10 I=1,NPT
      READ (1,1001) T(I),F(I),D(I),GA(I),GB(I)
      IF(D(I).EQ.0.) D(I)=D(I-1)
      IF(GA(I).EQ.0.) GA(I)=GA(I-1)
      IF(GB(I).EQ.0.) GB(I)=GB(I-1)
   10 CONTINUE
      DO 20 I=1,NPT
      X=D(I)/(F(I)*T(I)*GA(I)*GB(I)**2)
      TFA(I)=X
   20 TF(I)=10.*ALOG(X)/(2.303)
      WRITE (3,2000)
      WRITE (3,2001)(F(I),T(I),D(I),GB(I),GA(I),I=1,NPT)
      WRITE (3,2002)
      WRITE (3,2004) (F(I),TF(I),TFA(I),I=1,NPT)
      WRITE (2,3000) NPT
      WRITE (2,3001) (F(I),TF(I),I=1,NPT)
      GO TO 1
      END
```

APPENDIX E

Description and Explanation of the IBM-1410 Computer Program Used for Removal of the 60 cps Peak

This computer code was written to subtract the 60 cps peak from the power spectrum. Input to this code consisted of the number of points to be corrected, position of the 60 cps peak, power spectrum of the filter window, the number of data points, the frequency in cps and the power spectrum in decibels. Another input data card was added specifying the maximum and minimum value of the correcting constant k, and the value of Δk.

TABLE E-1. Variables required for the IBM computer code.

Symbol	Explanation
CON	Value of k
CONIM	Minimum value of k
CTF(I)	Corrected transfer function
DELCON	Increment of k
DIF	Difference between the input data power spectrum and the power spectrum of the filter window
F(I)	Frequency in cps
F(W)	Frequency in radians
FW(NP)	Power spectrum of the filter window
G(I)	Power spectrum in decibels
NC	Number of points to be corrected
NP	Position of the 60 cps peak
NPT	Number of data points

TABLE E-1 (continued)

Symbol	Explanation
TF(I)	Power spectrum in decibels
TPI	2 x π = 6.2831854
W(I)	Output frequency in radians

```
C       THIS PROGRAM REMOVES THE 60CPS PEAK FROM NOISE SPECTRUM
        DIMENSION F(50),TF(50),CTF(50),G(50),W(50),FW(14),FCOR(14)
 1000 FORMAT (12I6)
 1001 FORMAT (6F12.8)
 2000 FORMAT (6F12.6)
 3000 FORMAT (1HK,10X,27HCORRECTED TRANSFRE FUNCTION//15X,4HFREQ
     1,11X,2HT F,10X,6HCON = ,F10.6)
 3001 FORMAT (1H ,F21.8, F15.8)
        TPI=6.2831854
        READ (1,1000) NC,NP
        READ (1,1001) (FW(I),I=1,NC)
    2   READ (1,1000) NPT
        IF(NPT.EQ.0) CALL EXIT
        READ (1,1001) (F(I),TF(I),I=1,NPT)
        READ (1,1001) CON,CONMIN,DELCON
        DO 5 I=1,NPT
    5   TF(I)=TF(I)+100.
        DO 10 I=1,NPT
        IF(F(I).EQ.60.) GO TO 11
   10   CONTINUE
   11   ISIX=I
        DIF=TF(ISIX)-FW(NP)
        DO 20 I=1,NC
   20   FCOR(I)=FW(I)+DIF
    1   DO 25 I=1,NPT
   25   CTF(I)=TF(I)
        DO 30 I=1,NC
        I2=ISIX-NP+I
   30   CTF(I2)=TF(I2)-FCOR(I)*CON
        WRITE (3,3000) CON
        WRITE (3,3001) (F(I),CTF(I),I=1,NPT)
        WRITE (2,1000) NPT
        WRITE (2,2000) CON
        DO 40 I=1,NPT
        G(I)=CTF(I)-100.
        W(I)=TPI*F(I)
   40   WRITE (2,2000) G(I),W(I),F(I)
        X=CTF(1)-3.0
        DO 45 I=1,NPT
        IF(CTF(I).LE.X) GO TO 50
   45   CONTINUE
   50   WRITE (2,2000) W(I)
        CON=CON-DELCON
        IF(CON.LT.CONMIN)GO TO 2
        GO TO 1
        END
```

APPENDIX F

Description and Explanation of the IBM-1410 Computer Program Used for Calculation of the Break Frequency

This computer code was written to calculate the break frequency by a least squares fitting to the experimental points. Eqs. (C-5) through (C-7) were simultaneously solved by the Newton-Raphson iteration method (20).

Eqs. (C-5) and (C-6) were solved for A and B in terms of α and were considered as known quantities in the solution of Eq. (C-7), their values being calculated from the current value of α.

Eq. (C-7) was denoted by

$$\frac{\partial s}{\partial \alpha} = y(\alpha) \quad , \tag{F-1}$$

A Taylor series expansion of $y(\alpha)$ around the intital guess α_0 led to

$$y(\alpha) = 0 = y(\alpha_0) + (\alpha-\alpha_0) \cdot \frac{\partial y(\alpha_0)}{\partial \alpha} + \frac{(\alpha-\alpha_0)^2}{2!} \cdot \frac{\partial^2 y(\alpha_0)}{\partial \alpha^2} + \ldots \tag{F-2}$$

If the initial estimate α_0 is a good one the higher powers can be neglected. Thus

$$y(\alpha_0) - \Delta\alpha \cdot \frac{\partial y(\alpha_0)}{\partial \alpha} = 0 \tag{F-3}$$

where $\Delta\alpha = \alpha_0 - \alpha$.

Solving Eq. (F-3) for $\Delta\alpha$ yields

$$\Delta\alpha = \frac{y(\alpha_0)}{\frac{\partial y(\alpha_0)}{\partial \alpha}} \quad . \tag{F-4}$$

The derivative $\frac{\partial y(\alpha_0)}{\partial \alpha}$ was evaluated by the following numerical approximation:

$$\frac{\partial y(\alpha_0)}{\partial \alpha} = \frac{y(1.01\ \alpha_0) - y(\alpha_0)}{.01\ \alpha_0} \quad . \tag{F-5}$$

The next improved estimate for the break frequency was obtained by adding the correction factor $\Delta\alpha$. This new value of α was then used to calculate new values for A and B. The process was repeated till the iteration criterion was satisfied.

The Newton-Raphson iteration method was programmed in FORTRAN-IV language. The input of this program consisted of the number of data points, the experimental values for the power spectra, the corresponding frequencies and the initial guess for the break frequency.

The output of the program listed the least squares value for the break frequency, the least squares constant A and B, and the required information to plot the least squares fit to the experimental data.

TABLE F-1. Variables required for the IBM-1410 computer program.

Symbol	Explanation
A	White noise constant
A1	Corrected value for the white noise constant
ALPHA0	Initial guess for the break frequency
ALPHA1	Corrected value of the break frequency
AN(I)	Power spectrum in decibels
B	Pile noise constant
DALPH	Correction factor for the break frequency
DY	Numerical approximation for the derivative

TABLE F-1 (continued)

Symbol	Explanation
E	Iteration accuracy criterion
FA	First derivative with respect to A of the least squares curve
FAL	First derivative with respect to α of the least squares curve
FB	First derivative with respect to B of the least squares curve
N	Number of data points
W(I)	Angular frequency at which the data were analyzed
X	Least squares value for the break frequency
Y	Least squares function
YA	Corrected value for the least squares function
Z(I)	Power spectrum of the least squares fit in arbitrary units
ZZ(I)	Power spectrum of the least squares fit in decibels

```
C       THIS PROGRAM EVALUATES A LEAST SQUARE FIT TO THE DATA
C       POINTS
        DIMENSION AN(50),W(50),F(50),Z(50),ZZ(50)
      1 FORMAT (12I6)
      2 FORMAT (6F12.6)
     13 FORMAT(11X,7HERROR =,E14.8)
   3000 FORMAT (1H ,1PE18.6,3E15.6)
   3001 FORMAT (15HKERROR SQARED =,1PE12.5)
   3002 FORMAT (1H ,10X,4HGSQD,12X,1HW,14X,1HG,14X,2HAN)
   3003 FORMAT (3H1A=,1PE14.6/3H B=,F14.6/7H ALPHA=,E14.6/9H
       1GSQD(0)=,E16/5H CON=,E14.6)
   3004 FORMAT (9H ALPHAO =,F10.4,8H  TEST =,F10.5)
   3005 FORMAT (9HKBETA/L =,PE14.6/18H BREAK FREQUENCY
       1=,(PF6.3,4H CPS)
     71 READ(1,1)N
        IF(N.EQ.0) CALL EXIT
        READ (1,2) CON
        DO 10 I=1,N
     10 READ (1,2) AN(I),W(I),F(I)
        READ (1,2) ALPHA
        DO 20 I=1,N
     20 AN(I)=AN(I)+65.
        ALPHAO=ALPHA
     74 L=1
        WRITE (3,3004) ALPHAO,TEST
     75 X=ALPHAO**2
     76 AM=0.
        P=0.
        R=0.
        T=0.
        AJ=0.
        AL=0.
        DO 100 I=1,N
        AM=AM+AN(I)
        P=P+(1.)/(X+(W(I)**2))
        R=R+(AN(I))/(X+(W(I)**2))
        T=T+(1.)/((X+(W(I)**2))**2)
        AJ=AJ+(AN(I))/((X+(W(I)**2))**2)
    100 AL=AL+(1.)/((X+W(I)**2)**3)
        BN=N
        GO TO (110,150),L
    110 A=(R*P-AM*T)/(P*P-BN*T)
    120 B=(P*AM-R*BN)/(P*P-BN*T)
    130 Y=AJ-T*A-AL*B
```

REACTOR POWER CALIBRATION

BY NOISE ANALYSIS

by

JESUS LOPEZ-COTARELO VILLAAMIL

Perito Industrial, Escuela Tecnica de Madrid, 1961

AN ABSTRACT OF
A MASTER'S THESIS

submitted in partial fulfillment of the

requirements for the degree

MASTER OF SCIENCE

Department of Nuclear Engineering

KANSAS STATE UNIVERSITY

Manhattan, Kansas

1968

ABSTRACT

Noise analysis techniques were applied to the calculation of the power level at the KSUTMII reactor.

A preliminary step in power calibration is the determination of the zero power reactor transfer function, which was obtained from frequencies ranging from 2 cps to 1000 cps.

By a least squares fit of a function of the form $A + B/(\alpha^2 + \omega^2)$ to the experimental points, the break frequency was determined. The value obtained was 19.3 ± 0.6, which compares favorably with values obtained by other methods.

From the knowledge of the transfer function, the detector efficiency and the charge transferred per neutron absorbed were calculated. These two parameters are required for the calculation of the reactor power level. The values obtained are comparable to values obtained by other workers.

The reactor power was calibrated at several levels. Results are presented in tabulated form in the text. At low power levels the effects of instrument noise became important enough to override the pile noise. At high powers feedback temperature effects are present. The calculated power level was compared with the power indicated by the linear recorder of the reactor console. The results agreed within 20%.